6-30-2016

An Investigation of the Succination of the Selenoproteins Thioredoxin Reductase and Glutathione Peroxidase

Scott Lanci
University of South Carolina

An Investigation of the Succination of the Selenoproteins Thioredoxin Reductase and Glutathione Peroxidase

by

Scott Lanci

Bachelor of Science
Coastal Carolina University, 2012

Submitted in Partial Fulfillment of the Requirements

For the Degree of Master of Science in

Biomedical Science

School of Medicine

University of South Carolina

2016

Accepted by:

Norma Frizzell, Director of Thesis

Chandrashekhar Patel, Reader

Kenneth Walsh, Reader

Lacy Ford, Senior Vice Provost and Dean of Graduate Studies

DEDICATION

I would like to dedicate this thesis to my parents Jeff and Rose Lanci as well as my sister Jennifer Lanci. My family has always given me their unwavering support as I have pursued my dreams. My mentor Dr. Norma Frizzell has also given me the tremendous opportunity to work in her laboratory to obtain my Master's Degree at the University of South Carolina School of Medicine, for which I will always be grateful.

ACKNOWLEDGEMENTS

I would like to thank my mentor, Dr. Norma Frizzell, above all for graciously allowing me to work in her laboratory to pursue my Master's Degree. I would like to give special thanks to Dr. Gerardo Piroli for his contributions to my project and his expertise and advice throughout my time working in this lab. I would also like to thank our current Ph.D. student Allison Manuel, our current M.S. student Lydia Proctor, and our laboratory technician Anna Clapper for their individual contributions to my project and for teaching me new laboratory techniques.

ABSTRACT

We have identified the irreversible protein modification S-(2-succino)cysteine, a product of the Kreb's cycle intermediate fumarate reacting with the thiol group of cysteine (Cys) residues, also termed *succination*. Succination is increased in adipose tissue of diabetic mice *in vivo* and in adipocytes matured in high glucose medium (25 mM) *in vitro*. Selenocysteine (Sec) is a less common but highly conserved amino acid that has major functions in redox chemistry. Sec possesses a lower pK_a (~5.4) and is much more reactive in comparison to Cys. This project aimed to determine if succination occurred on Sec residues in two selenoproteins that play roles of maintaining intracellular redox environments and contain Sec in their active sites, thioredoxin reductase (TrxR) and glutathione peroxidase (GPx). We hypothesized that increased fumarate levels will lead to the succination of Sec and causing decreased enzymatic activity for each enzyme.

Two cellular models were used with elevated fumarate levels: (1) 3T3-L1 adipocytes matured in high glucose medium (25 mM) to mimic diabetic conditions and (2) 3T3-L1 fibroblasts where fumarase was knocked-down (*Fh* k/d) to mimic fumarase deficient cancers. As a positive control to demonstrate the ability to succinate TrxR *in vitro*, recombinant TrxR1 was incubated with the reactive fumarate ester, dimethyl fumarate (DMF). After analysis, a ~56% reduction in activity was detected due to succination of an active site residue, which was confirmed by mass spectrometric analyses.

Unexpectedly, TrxR activity was found to be significantly increased in 3T3-L1 adipocytes matured in 25 mM glucose compared to 5 mM glucose, despite no changes in protein levels. No statistically significant changes in TrxR activity were found in *Fh* k/d 3T3-L1 fibroblasts compared to controls. GPx activity was found to be significantly reduced in 3T3-L1 adipocytes matured in high glucose with no changes in levels of GPx protein. GPx activity was also analyzed in *Fh* k/d 3T3-L1 fibroblasts, however no significant changes were detected.

Overall, the results demonstrate that TrxR can be modified readily by reactive fumarate esters, leading to decreased enzymatic activity. However, endogenously produced fumarate does not appear to significantly contribute to TrxR or GPx modification in the models studied.

TABLE OF CONTENTS

LIST OF TABLES

LIST OF FIGURES

LIST OF ABBREVIATIONS

2SC.....S-(2-succino)cysteine

4-VP 4-vinylpyridine

AF .....Acylfulvene

ARE.....Antioxidant Response Element

ASK1..... Apoptosis Signal-Regulated Kinase 1

ATM..... Aurothiomalate

DMEM ..... Dulbecco's Modified Eagles Medium

DMF ..... Dimethyl Fumarate

DTNB.....5,5'-dithio-*bis*(2-dinitrobenzoic acid)

DTT.....Dithiothreitol

EDTA ..... Ethylenediaminetetraacetic Acid

FAD..... Flavin Adenine Dinucleotide

Fh .....Fumarase

GAPDH..... Glyceraldehyde-3-phosphate Dehydrogenase

GF ..... Growth Factor

GPx ..... Glutathione Peroxidase

GR..... Glutathione Reductase

GSH.....Glutathione

HLRCC .....Hereditary Leiomyomatosis and Renal Cell Cancer

HNE ..... Hydroxy-nonenal

HO-1 ..... Heme Oxygenase 1

Keap1 ..... Kelch-like ECH-associated Protein 1

LC-MS/MS .....Liquid Chromatography/Mass Spectrometry

MMF .....Monomethyl Fumarate

MRI .....Magnetic Resonance Imaging

MS..... Multiple Sclerosis

NADH .....Nicotinamide Adenine Dinucleotide

NADPH..... Nicotinamide Adenine Dinucleotide Phosphate

NO..... Nitric Oxide

Nrf2 .....Nuclear Factor (erythroid-derived)-like 2

Park7 .....Parkinson Disease Protein 7

PTEN..... Phosphatase and Tensin Homolog

PVDF .....Polyvinylidene Fluoride

RNS..... Reactive Nitrogen Species

ROS.....Reactive Oxygen Species

RRMS ..... Relapsing-Remitting Multiple Sclerosis

SDS-PAGE ..... Sodium Dodecyl Sulfate Polyacrylamide Gel Electrophoresis

SECIS..... Selenocysteine Insertion Sequence

Trx.....Thioredoxin

TrxR ..... Thioredoxin Reductase

Txnip .....Thioredoxin Interacting Protein

CHAPTER 1

GENERAL INTRODUCTION

1.1 Succination of Proteins

The amino acid cysteine (Cys) plays unique biological roles in nature due to its chemical structure. Cysteine contains a thiol group with a pK_a ~9.5 (1) when exposed on the surface of a protein, but its pK_a can be as low as ~3-4 when located within the active site of an enzyme (2). Therefore the thiol group is readily deprotonated in physiological conditions and can be considered one of the most reactive residues found in peptides (3). This reactivity makes cysteine a strong nucleophile and the thiolate (S^-) is susceptible to increased oxidation to the reversible sulfenic acid (SOH) (4), or further to the irreversible sulfinic ($S(O)_2H$) and sulfonic acids ($S(O)_3H$) (5). Sacrificial thiol oxidation is known to play an important role in the cellular response to oxidative stress, and partially oxidized thiols are often functionally regenerated by the glutathione system.

Alterations in cellular metabolism may lead to increases in oxidizing intermediates, but other metabolic intermediates are also capable of chemically modifying cysteine thiolates. Recently, the modification of cysteine residues in proteins by the Kreb's cycle intermediate fumarate has been described. In the case of this modification, known as protein succination, fumarate undergoes a Michael addition reaction to form a thioether bond with the thiol group of cysteine yielding a product termed S-(2-succino)cysteine (2SC) (6, 7) (Figure 1.1). Protein succination is an

irreversible, non-enzymatic post-translational modification of proteins that may result in alteration of the protein structure or function. The 2SC modification has been detected on over 50 proteins expressed by mouse adipocytes (6), but has also been detected in human plasma albumin, consisting of 3.5% of the total protein (7), in skin collagen and skeletal muscle proteins (2). Reduced functionality following protein succination has been demonstrated for cytosolic glyceraldehyde-3-phosphate dehydrogenase (GAPDH) and mitochondrial aconitase, with both exhibiting decreased enzymatic activity (8, 9). GAPDH is a glycolytic enzyme that, when inhibited during hyperglycemic conditions, is linked to the development of diabetic complications such as vascular endothelial damage (10). Aconitase is a Kreb's cycle enzyme responsible for isomerization of citrate to isocitrate and its impaired activity results in a disruption in mitochondrial metabolism (9). The adipocyte hormone adiponectin circulates in plasma as high molecular weight oligomers and stimulates fatty-acid oxidation in muscle and in the liver (11). Adiponectin is also a target of succination and this inhibits its oligomerization, preventing its secretion into plasma where it can circulate to its target receptors throughout the body (12). This fact is significant considering that high molecular weight forms of adiponectin are decreased in the plasma of Type 2 diabetics.

In the adipocyte, protein succination is a direct effect of mitochondrial stress caused by elevated extracellular glucose levels when cellular metabolism is increased. These conditions lead to an increase in ATP/ADP ratios and an accumulation of ATP. This accumulation inhibits the mitochondrial electron transport chain through respiratory control, increasing the mitochondrial membrane potential ($\Delta\psi_m$) and NADH/NAD^+ ratio, leading to an accumulation of fumarate due to the inhibition of NAD^+–dependent Kreb's

cycle enzymes (13) (Figure 1.2). Increased levels of succinated proteins have been demonstrated in both 3T3-L1 adipocytes matured in high glucose medium (30 mM) versus normal glucose medium (5 mM), and in the adipose tissue of diabetic *db/db* mice (13, 14). Beyond the adipocyte, increased succination has also been detected in hereditary leiomyomatosis and renal cell cancer (HLRCC) where the enzyme fumarase, responsible for converting fumarate to malate, is deficient or mutated, leading to a pronounced increase in succination in these tumors (15). In fact, the immunohistochemical detection of succinated proteins is used clinically as a biomarker for fumarase deficiency (6, 16, 17, 18). Increased levels of protein succination have most recently been described in a mitochondrial encephalopathy associated with a defect in mitochondrial oxidative phosphorylation, where increased succination of select proteins may play a role in defective neuronal function (19).

1.2 Selenocysteines

In general, there are twenty abundant amino acids found in nature. However a less common, but highly conserved amino acid, selenocysteine (Sec), plays a critical role in a range of cellular functions. Often coined the "21st amino acid" (20), Sec has a similar chemical structure to the more common amino acid cysteine, with the exception of a selenium atom in place of sulfur. The two amino acids have different chemical properties, as selenocysteine has a much lower pK_a value (~5.4) compared to cysteine (~9.5) (21). This lower pK_a of Sec results in the selenol group (SeH) being deprotonated in physiological pH ranges (6.5-7.5), yielding the selenolate (Se^-) form, and thus Sec is more reactive than Cys (22). Sec is inherently a strong nucleophile, and therefore is often found in the active site of enzymes that play a role in redox reactions.

Selenoproteins are defined as proteins that contain one or more Sec in their sequence. During protein translation, Sec is encoded by the UGA mRNA codon, which under normal circumstances will terminate protein synthesis (23). However the mRNAs for selenoproteins contain a selenocysteine insertion sequence (SECIS), a stem-loop structure that resides downstream from the UGA codon and allows the Sec-specific translation machinery to associate with the ribosome (20). Without the SECIS, the protein will be prematurely truncated and no Sec will be incorporated.

Selenoproteins exist in all three domains of life and currently over 50 different families of these proteins have been identified (24). Humans contain 25 known genes that encode selenoproteins (23), having functions from redox signaling, protection from reactive oxygen species (ROS), protein folding and thyroid hormone metabolism. The wide range of biological functions that selenoproteins possess, particularly in redox biology, is dependent upon the chemical properties of selenocysteine (24). These proteins are widely distributed throughout the human body, some being ubiquitous while others are tissue and organelle specific (25). Many selenoproteins are proposed to be essential for normal brain development and therefore highly expressed in nervous system, and deficits in some selenoproteins have been linked to an assortment of neurological disorders in mice (26, 27, 28).

1.3 Oxidative Stress in Disease

Reactive oxygen species (ROS) can arise in the cell from mitochondrial oxidative metabolism, or from cellular responses to xenobiotics, cytokines or microbial invasion (29). The most abundant forms of these species found in the cell are hydrogen peroxide

(H_2O_2) or superoxide (O_2^-). Under physiological concentrations, ROS may function as regulators of intracellular signaling pathways, primarily through the oxidative modification of specific cysteine residues on target proteins (30). In some cases, ROS have significant physiological roles, for instance they are involved in the regulation of cellular processes such as inflammation through modification of Nuclear Factor kappa B thiol groups (31, 32), and the response to growth factor (GF) stimulation (30). Maintaining an appropriate concentration of ROS is critical for normal cellular function, and oxidant mediated stress may develop when the production of ROS increases. Therefore antioxidant systems such as the thioredoxin and glutathione systems must also be properly regulated to maintain homeostatic environments. The abundance of Sec containing selenoproteins in the antioxidant response system emphasizes the roles of these proteins in dealing with the balance of intracellular ROS.

Oxidative stress is defined as a disruption in the balance between the production of ROS and antioxidant defenses (33). Therefore, oxidative stress can arise when there is an increase in the amount of ROS produced and/or a decrease in the activity or levels of antioxidants (34). In diseases such as diabetes mellitus, hyperglycemic conditions lead to a pronounced increase in the production of ROS, disrupting the physiological balance between oxidants and antioxidants, ultimately causing oxidative stress and cellular damage (35). Adipocytes exposed to hyperglycemic conditions *in vitro* and *in vivo* are associated with increased levels of ROS production, a pronounced inflammatory response and insulin resistance (36). Insulin resistance in skeletal muscle has been linked to persistently oxidized redox environments caused by increased mitochondrial ROS production during high fat diet feeding (37). The thioredoxin system, specifically

thioredoxin reductase 1 (TrxR1), has been shown to be critical for neutralizing glucose-derived H_2O_2 under high glucose conditions *in vitro* (38).

1.4 Thioredoxin Reductase

The thioredoxin system, consisting of thioredoxin (Trx), thioredoxin reductase (TrxR) and nicotinamide adenine dinucleotide phosphate (NADPH), is ubiquitous in all cellular organisms (39). This crucial system provides redox regulation of protein function and signaling through its action of reducing cellular thiols (39). Wide regulation of gene expression through redox control of transcription factors constitutes one of the major roles of the thioredoxin system (40). Trx, in its reduced form, serves as a hydrogen donor to catalyze the reduction of disulfide bonds found in the redox-sensitive proteins such as apoptosis signal-regulated kinase 1 (ASK1), thioredoxin interacting protein (Txnip), phosphatase and tensin homolog (PTEN), and other targets that function in the modulation of cellular processes such as inflammation, metabolism, development, proliferation and migration (41). Through maintaining intracellular redox environments, this system also provides a major defense against oxidative stress and the prevention of apoptosis (42).

Thioredoxin reductase is also a critical part of the thioredoxin system as its primary function is to maintain the reduced form of Trx through its catalytic cycle (39) (Figure 1.3). TrxR is a monomeric selenoprotein, with the active site Sec residue located penultimate to the C-terminal glycine of the protein (40, 43). The N-terminal region of TrxR is an FAD (flavin adenine dinucleotide)-binding domain, which is responsible for the transfer of reducing equivalents in the catalytic cycle (44). During TrxR catalysis,

electrons are transferred from NADPH to the TrxR-bound FAD, which subsequently transfers electrons to reduce the active site Cys-Sec selenylsulfide bond (40, 44). The importance of the active site Sec during the TrxR catalytic cycle is highlighted when this residue is substituted with Cys, as this does not result in the formation of an active site disulfide bond and the Cys mutant enzyme shows almost no activity (38, 40, 43). Three mammalian forms of TrxR have been identified: the cytosolic TrxR1, the mitochondrial TrxR2, and the testis-specific TrxR3 (40), with the most abundant isoforms being TrxR1 and TrxR2.

In its reduced form, TrxR has the ability to directly reduce other substrates inside the cell, both proteins and small molecules such as vitamin K, alloxan and lipoic acid (40). As previously mentioned Sec has a pK_a ~5.4 and will be ionized under physiological pH ranges. The reactivity of Sec and its exposed location on TrxR leaves the enzyme susceptible to modification at the active site, rendering it incapable of reductase activity. Modification of TrxR has previously been demonstrated *in vitro* by exogenous electrophiles where the Sec residue and several other Cys residues were irreversibly modified (45, 46).

1.5 Glutathione Peroxidase

The glutathione system consists of the enzymes glutathione (GSH), glutathione reductase (GR), glutathione peroxidase (GPx), and the hydrogen donor NADPH. GSH contains a thiol group in the form of a cysteine residue and plays a major role in the cellular antioxidant response through either the direct reduction of reactive oxygen/nitrogen species (ROS/RNS), or by acting as a cofactor for other enzymes (47).

The reduced form of glutathione (GSH) becomes oxidized to GSSG following the reduction of cellular proteins or the neutralization of hydrogen peroxide (H_2O_2). This system is considered to be the back-up for the thioredoxin system that also serves to protect from oxidative damage, as previously described.

Glutathione peroxidase is a key selenoprotein in this system's regulation of redox environments, containing a Sec residue in its active site. The properties of Sec allow GPx to function as a strong reducing agent and it is involved in the reduction of hydrogen peroxides, organic hydroperoxides (e.g. cumene hydroperoxide) and lipid peroxides from fatty acid radicals (24). In the catalytic cycle for the neutralization of H_2O_2, the selenolate (Se^-) group reacts with H_2O_2 to form selenic acid (SeOH), which is subsequently reduced back to selenol (SeH) by 2 GSH, yielding GSSG and water (48, 49, 50, 51) (Figure 1.4). GSSG is reduced by the enzyme glutathione reductase through the transfer of hydrogen from NADPH, recycling the system and allowing it to repeat its redox activity. The first isoform of GPx (GPx1) was the first human selenoenzyme to be discovered (52). There are a total of 8 identified isoforms of this enzyme; however GPx1 and GPx4 are the most abundant and ubiquitously expressed isoforms in the cell (51).

The neutralization of H_2O_2 allows GPx1 to maintain the balance between the required concentrations of ROS that play physiological roles and the higher concentrations that lead to cellular damage (53). GPx4 has a more specialized function of protection of membranes from lipid peroxidation directly by hydroperoxides found inside of membranes; a function that enables this isoform of the enzyme to be involved in the attenuation of oxidative stress-induced apoptosis (24, 51). Alterations in the levels or the activity of GPx can lead to abnormal levels of intracellular ROS and these changes have

been linked to cardiovascular disease and diabetes (53). There are no known specific inhibitors of GPx, however oxidative modification of thiols and selenols represents the most characterized modification of this enzyme (53).

1.6 Research Hypothesis and Aims

Due to the chemical nature of selenocysteine and its predicted higher reactivity at physiological pH when compared to cysteine, I hypothesize that Sec is susceptible to succination when fumarate levels are elevated. Preliminary experiments in our lab have demonstrated that free amino acid Sec can be succinated by fumarate following *in vitro* incubation (unpublished data). Although this *in vitro* experiment does not account for the variable factors that can affect the reactivity of a protein, it provides a foundation for the aims of this thesis further described in the hypothesis. The fact that lower pK_a residues in proteins may be more vulnerable to this modification has been demonstrated following the identification of succination of Parkinson disease protein 7 (Park7) on an active site Cys that possesses an unusually low pK_a (~5.4) (16). In this thesis I will examine the succination of the selenoproteins thioredoxin reductase and glutathione peroxidase. Due to the presence of Sec in the active site of these enzymes, irreversible modification of this residue is predicted to inhibit the enzyme. As a consequence, the resulting decreased activity may leave the cell more vulnerable to redox active species. The exposed location of Sec on the C-terminus of TrxR makes this protein particularly interesting as a candidate for succination.

Two different cell culture models will be used in this investigation; (1) adipocytes matured in high glucose medium to model diabetic conditions (versus controls in normal

glucose medium), or (2) fumarase knockdown in fibroblasts to model fumarase-deficient cancers, creating a model of enhanced succination. I will specifically examine the activity and protein levels of thioredoxin reductase and glutathione peroxidase in both of these cell models of elevated endogenous fumarate.

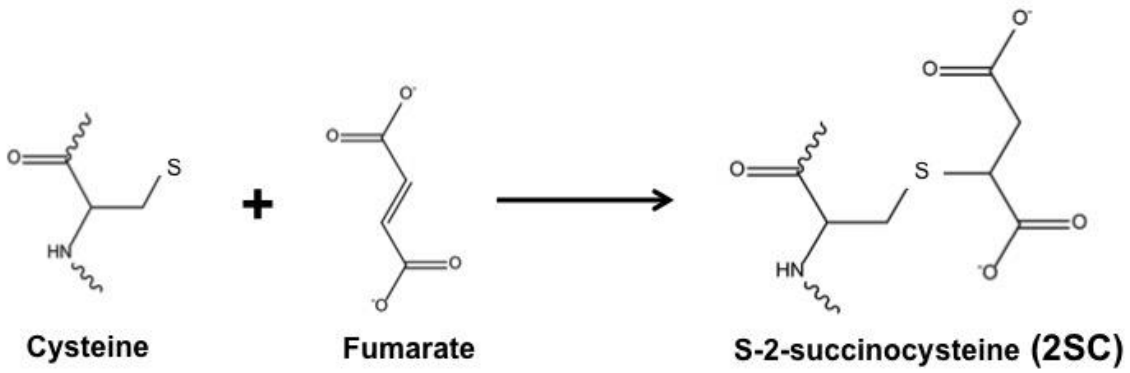

Figure 1.1: Protein succination reaction mechanism. Fumarate undergoes a Michael addition reaction to form a thioether bond with the thiol group of cysteine residues, yielding a product termed S-(2-succino)cysteine (2SC). Protein succination is an irreversible, non-enzymatic post-translational modification of proteins that may result in alteration of the protein structure or function.

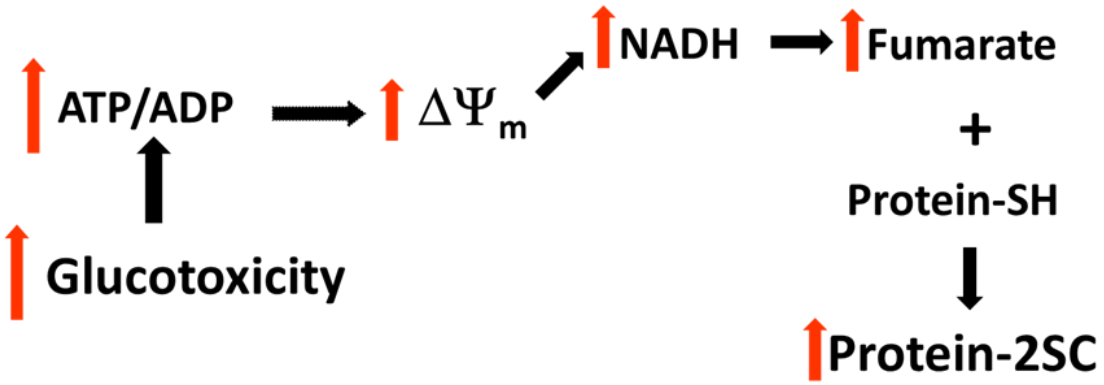

Figure 1.2: Glucotoxicity driven mitochondrial stress increases protein succination. In the adipocyte, protein succination is a direct effect of mitochondrial stress caused by elevated extracellular glucose levels when cellular metabolism is increased. These conditions lead to an increase in ATP/ADP ratios and an accumulation of ATP. This accumulation inhibits the mitochondrial electron transport chain through respiratory control, and increasing the mitochondrial membrane potential ($\Delta\psi_m$) and NADH/NAD^+ ratio, leading to an accumulation of fumarate due to the inhibition of NAD^+–dependent Kreb's cycle enzymes. Elevated levels of intracellular fumarate lead to the succination of protein thiols.

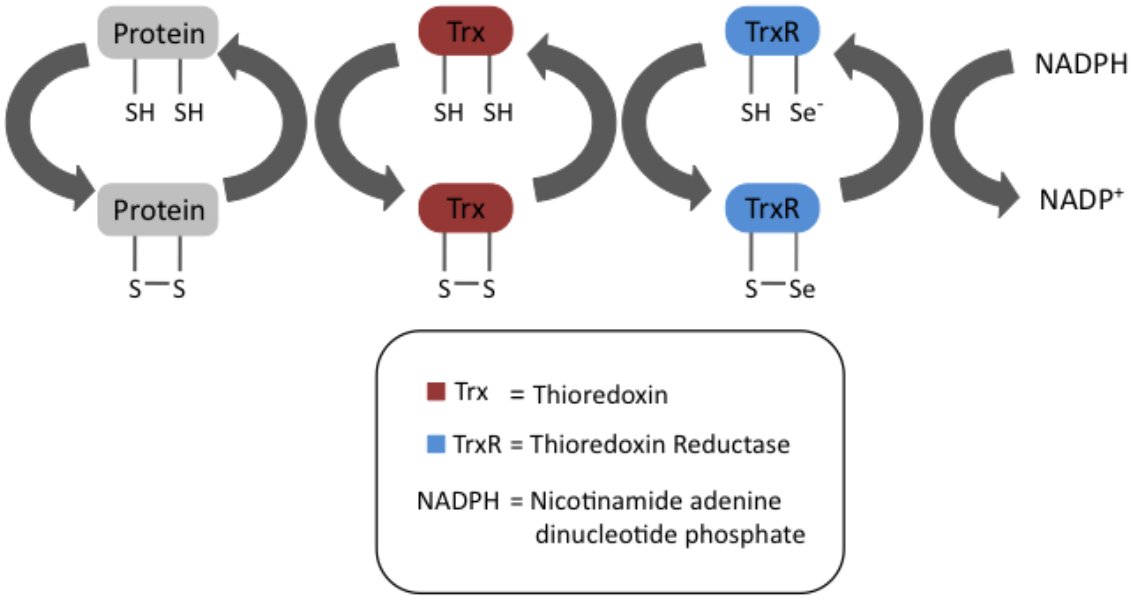

Figure 1.3: The Thioredoxin system. The thioredoxin system consists of thioredoxin (Trx), thioredoxin reductase (TrxR) and the hydrogen donor nicotinamide adenine dinucleotide phosphate (NADPH). This ubiquitous system provides redox regulation of protein function and signaling through its action of reducing cellular thiols. TrxR is a selenoprotein containing a selenocysteine (Sec) in its active site, and it is responsible for reducing the disulfide bond in Trx.

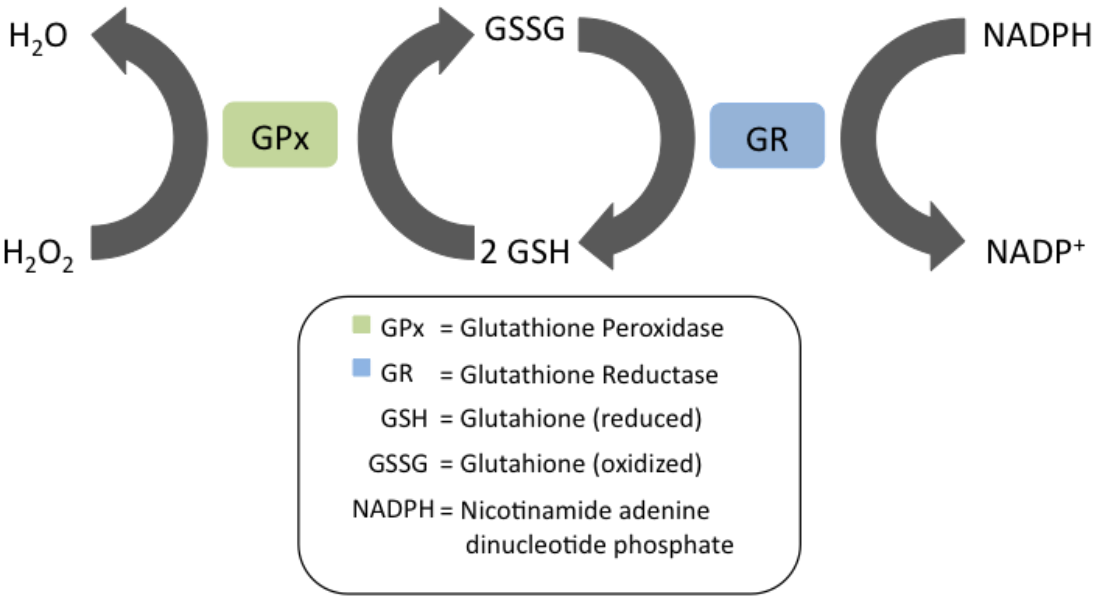

Figure 1.4: The Glutathione system. The glutathione system consists of the enzymes glutathione (GSH), glutathione reductase (GR), glutathione peroxidase (GPx), and the hydrogen donor nicotinamide adenine dinucleotide phosphate (NADPH). GSH contains a thiol group in the form of a cysteine residue and plays a major role in the cellular antioxidant response through either the direct reduction of reactive oxygen/nitrogen species (ROS/RNS), or by acting as a cofactor for other enzymes such as GPx. GPx is a scavenging selenoprotein containing a selenocysteine (Sec) in its active site, and it plays vital protective roles inside the cell through its function of reducing damaging species such as hydrogen peroxide (H_2O_2), organic peroxides and lipid peroxides.

CHAPTER 2

THE EFFECTS OF DIMETHYL FUMARATE (DMF) AND FUMARATE ON THIOREDOXIN REDUCTASE 1

2.1 Introduction

Multiple sclerosis (MS) is an inflammatory disease that results in the demyelination and loss of axons in the central nervous system (CNS) (54). The disease affects approximately one in every thousand Americans; with females being affected twice as often as males (55, 56). Tecfidera® is a recently approved drug used to treat relapsing-remitting MS (RRMS), a form of the disease characterized by attacks of worsening neurological function, followed by partial or complete recovery periods (57). The primary active component of Tecfidera® is dimethyl fumarate (DMF), a more reactive fumarate ester that is more easily absorbed and has better bioavailability than fumarate when administered orally (58, 59). DMF is also considered both safe and effective in the treatment of psoriasis, where it has been approved for use in Europe for over a decade (60). After ingestion, intracellular esterases rapidly hydrolyze DMF to the bioactive metabolite monomethyl fumarate (MMF) (58, 61). The efficacy of DMF treatment was tested in two randomized, double-blind, placebo-controlled clinical trials with RRMS patients and resulted in significantly reduced lesions (permanent axonal damage/loss), confirmed by magnetic resonance imaging (MRI) in those individuals who received the drug (58, 62, 63, 64, 65).

DMF promotes therapeutic cytoprotection in treating RRMS through the activation of the nuclear factor (erythyroid-derived)-like-2 (Nrf2) pathway, a transcription factor that induces the upregulation of antioxidant proteins (66, 67). After DMF is metabolized to MMF, it reacts with a Cys residue on the Nrf2-bound Kelch-like ECH-associated protein 1 (Keap1), leading to the stabilization of Nrf2 and its translocation to the nucleus where it binds the antioxidant response element (ARE) and promotes the transcription of its target antioxidant genes such as gamma-glutamylcysteine synthetase (synthesizes glutathione (GSH)) and thioredoxin reductase 1 (TrxR1) (68, 69). DMF/MMF readily reacts with the cysteine thiol of GSH, one of the first described targets of the drug, causing levels to be depleted and strongly inducing the anti-inflammatory stress protein heme oxygenase 1 (HO-1) (70, 71). DMF also suppresses pro-inflammatory genes by inhibiting nuclear factor kappa B, and combined with the anti-oxidative targets of Nrf2 activation, these responses are believed to slow the demyelination and neurodegeneration associated with MS by causing a decrease in circulating T cells and $CD4^+$ cells involved in inflammation (62, 66, 72, 73).

Despite the efficacy of DMF treatment in MS patients and the increased quality of life observed after clinical trials, the drug is also known to cause side effects such as gastrointestinal discomfort, nausea and flushing severe enough for ~10% of patients to discontinue use (73). The presence of these side effects and the inherent reactivity of fumarate esters would suggest that there are other cellular targets that are also being modified. Our laboratory has recently confirmed that DMF and its metabolite MMF result in the succination of multiple proteins in 3T3-L1 mouse adipocytes treated with DMF (74). Pronounced increases in succinated Cys residues were also identified

following immunoblotting and LC-MS/MS analysis of porcine tubulin treated with DMF, and increased succination prevented its polymerization (75).

As previously mentioned, the Cys-Sec residues in the active site of TrxR reside on the exposed C-terminal region of the protein (Figure 2.1), suggesting this region of TrxR may be a likely target of DMF modification. In this study I investigated the succination of TrxR by DMF, hypothesizing that (1) I would demonstrate the vulnerability of this enzyme's active site to modification and, (2) identify a novel protein modified by DMF. These studies would also determine if the same active site residues might also be susceptible to succination by the less reactive but endogenously produced metabolite fumarate.

2.2 Results

To determine the effects of DMF on TrxR activity *in vitro*, rat recombinant thioredoxin reductase 1 (TrxR1) protein was reduced with NADPH prior to incubations with 0, 5, 50 and 100 µM DMF for 1 hour at room temperature. The pre-reduction step of TrxR by NADPH is necessary since the active site Cys-Sec forms a selenylsulfide bond (Figure 1.3) (46), needs to be reduced so that the selenolate (Se^-) can react with electrophiles. The enzymatic activity was measured following the reduction of 5 mM 5,5'-dithio-*bis*(2-dinitrobenzoic acid) (DTNB) and expressed as the rate of molar nicotinamide adenine dinucleotide phosphate (NADPH) oxidation per mg protein (mean ± S.E.M) (Figure 2.2). Incubations with 50 and 100 µM DMF exhibited activities (mean ± S.E.M.) of 9.98 ± 0.41 and 5.71 ± 0.24 µmol/min/mg respectively, compared to the control activity of 13.74 ± 0.54 µmol/min/mg. These activities were statistically

significant decreases compared to the control; a ~27% average decrease in activity for the 50 µM group and ~56% average decrease in the 100 µM group.

Proteomic analysis using high-resolution mass spectrometry (MS) was performed on rat recombinant TrxR1 incubated in 100 µM DMF for 1 hour at room temperature to confirm succination and also identify specific succinated residues. The protein was digested with trypsin (cleaves after lysine and arginine residues), generating a series of peptides that were distinguished based on the mass/charge ratio (m/z). The potential alteration in peptide mass due to the addition of MMF or DMF protein adducts on Cys or Sec residues was then considered. This analysis revealed that DMF modified 3 of the 13 Cys residues on the protein; Cys177 was modified by MMF, Cys189 was modified by either MMF or DMF, and Cys475 was modified by MMF. All of these cysteine containing peptides were detected with increases in mass of 130 Da (mass of MMF) or 144 Da (mass of DMF). The masses detected were consistent with the Michael addition of free cysteine sulfhydryl group across the double bond of MMF or DMF. Despite the immediate identification of several succinated cysteine containing peptides, I was particularly interested in the N-terminal peptide containing the Sec residue. Further MS/MS analysis and fragmentation of the specific mass attributed to the terminal peptide sequence (SGGDILQSGCUG) confirmed MMF modification of this peptide. However, while the ion fragments detected confirmed the identity of the succinated peptide, they did not allow the assignment of the specific succinated site, i.e. it was either one of active site residues Cys497 or U498 (Table 2.1). An MS/MS spectrum of the peptide ($[MH+3]^{3+}$, 458.50 Daltons) (Figure 2.3) shows the 5 fragments of the parent ion identified and the corresponding masses, confirming sequence identity. The fragments

detected are b ions, indicating they were generated from the fragmentation at the N-terminus of the peptide. The data confirms that the active site Sec containing peptide was succinated, amongst additional succinated sites, in association with the reduction in enzymatic activity.

After successfully demonstrating reduced activity of TrxR1 *in vitro* by succination of active site residues after DMF treatment, the effects of fumarate on the enzymatic activity were investigated. Recombinant rat TrxR1 protein was pre-reduced with NADPH prior to incubations with 0, 10, 50 or 100 mM fumarate for 6 hours at room temperature. TrxR activity was measured and expressed as the rate of molar NADPH oxidation per mg protein (mean ± S.E.M). However there was no detectable reduction in enzymatic activity with any fumarate concentration compared to the control group (Figure 2.4). Additional experiments were performed at a range of different incubation times and temperatures; however detectable decreases in TrxR activity could not be established (data not shown).

TrxR activity and protein levels were next investigated in the lysates of N1E-115 neuronal cells after treatment with DMF. The cells were treated with a 100 µM DMF for either 3 hours or 24 hours prior to harvesting protein, and compared to a control group where no DMF was added. However, reliable data for TrxR activity could not be generated for this model. The TrxR activity assay utilizes a TrxR-specific inhibitor, where the total thiol-reducing activity (samples without inhibitor) is measured in parallel with the non-TrxR thiol reducing activity (samples containing TrxR inhibitor). TrxR activity can be calculated by subtracting the non-TrxR activity (inhibitor present) from the total thiol-reducing activity (inhibitor not present). Two separate attempts at this

assay were performed however samples containing the TrxR inhibitor consistently displayed higher activities than the non-inhibited samples, resulting in negative values for TrxR activity. In the absence of TrxR activity, the total protein levels of TrxR1 and TrxR2 were analyzed in the control vs. 3 hour DMF vs. 24 hour DMF by immunoblotting, however no apparent changes in the levels of the cytoplasmic TrxR1 (Figure 2.5, TrxR1 panel, lanes 1-5 vs. lanes 6-10 vs. lanes 11-15) or mitochondrial TrxR2 (Figure 2.5, TrxR2 panel) were detected between the three groups. The levels of α-tubulin (DM1A) were used to demonstrate equal protein loading (Figure 2.5, DM1A panel).

2.3 Discussion

The ability of DMF to modify TrxR and significantly reduce its activity was confirmed through enzymatic activity assays and MS proteomic analysis. This is the first time that succination has been identified as a modification of this enzyme and these data provide new information on the mechanism of action of this drug. The reactivity of DMF is also highlighted by these findings, as the protein was modified with reduced activity after only 1 hour incubation at room temperature, and these results served as proof of concept for the susceptibility of TrxR to succination. Although MS/MS analysis could not confirm succination of the particular succinated residue in the active site (Cys497 or Sec498, Table 2.1), the observed decrease in enzymatic activity was most likely due to the modification of either active site residue by DMF, since they are both critical for the overall reaction mechanism (Figure 1.3). One might postulate that the much higher reactivity of Sec compared to Cys would cause Sec to be more favorably modified. Despite the uncertainty surround the particular active site residue was modified by DMF,

the data clearly demonstrates that a reduction in enzymatic activity could be observed after modification of either of these residues. Future experiments may be able to confirm the precise location of modification through further MS analysis to determine if Sec specifically has greater reactivity with this electrophile.

Although succination and decreased TrxR activity was observed *in vitro* for recombinant protein treated with DMF, the inability to successfully measure TrxR activity in a cell treated with DMF does not allow further conclusions to be drawn regarding DMF effects on intracellular TrxR. The TrxR activity assay utilizes a TrxR inhibitor (sodium aurothiomalate) that allows other non-TrxR enzymatic reductions of DTNB to be subtracted from the total activity measured. Two activity experiments were performed on N1E-115 cell samples where groups with the inhibitor present abnormally resulted in higher activities in comparison to where the inhibitor was not present. This did not allow a positive value of TrxR activity to be calculated for these samples.

This was disappointing since it might be expected that decreased TrxR activity, even transiently, in the cell might be due to the chemical modification of the enzyme by DMF treatment. We chose to examine the effect of DMF in a neuronal cell that was already available in our laboratory for other studies. Since DMF is used to treat RRMS, any alterations in TrxR activity (whether transient or prolonged) might assist in explaining an aspect of the beneficial or side effects of this drug. We would hypothesize that DMF treatment would reduce enzymatic activity, prompting an increase in oxidative stress that would result in Nrf2 activation and an increased production of cellular antioxidant proteins (see Chapter 2 *Introduction*). Modification of TrxR by DMF may be a transient and necessary component of inducing a stronger and improved antioxidant

balance in the cells. Immunoblotting of the protein lysates from the treated cells demonstrated that neither levels of TrxR1 nor TrxR2 had changed in the control or DMF-treated groups (Figure 2.5, TrxR1 and TrxR2 panels). However, due to the inability to measure TrxR activity in these cells, the protein levels cannot be correlated with enzymatic activities at this time. Therefore, we look forward to future experiments involving this cellular model again while utilizing an alternative commercially available TrxR activity assay to determine the time dependency of DMF-induced decreases in enzymatic activity. Overall, the preliminary investigations in the studies described confirmed that fumarate, at least a reactive fumarate ester, could modify the active site of TrxR.

In contrast, the inability to detect changes in the recombinant TrxR1 activity after treatment with fumarate may be due to the decreased reactivity of this metabolite versus DMF. Despite performing repeated experiments with varying incubation times and temperatures, consistent changes in TrxR activity could not be detected. It may also be the case that succination of this protein by fumarate is not detectable in this *in vitro* time frame. The results of these experiments led me to conclude that I should examine the effects of elevated fumarate levels on TrxR in cellular models. Cells can provide a more suitable environment for proteins to be exposed to endogenously produced fumarate for longer periods of time, and these conditions could provide a better environment to observe the succination of TrxR.

```
        10         20         30         40         50
MNDSKDAPKS YDFDLIIIGG GSGGLAAAKE AAKFDKKVMV LDFVTPTPLG
        60         70         80         90        100
TRWGLGGTCV NVGCIPKKLM HQAALLGQAL KDSRNYGWKL EDTVKHDWEK
       110        120        130        140        150
MTESVQNHIG SLNWGYRVAL REKKVVYENA YGKFIGPHKI MATNNKGKEK
       160        170        180        190        200
VYSAERFLIA TGERPRYLGI PGDKEYCISS DDLFSLPYCP GKTLVVGASY
       210        220        230        240        250
VALECAGFLA GIGLDVTVMV RSILLRGFDQ DMANKIGEHM EEHGIKFIRQ
       260        270        280        290        300
FVPTKIEQIE AGTPGRLKVT AKSTNSEETI EDEFNTVLLA VGRDSCTRTI
       310        320        330        340        350
GLETVGVKIN EKTGKIPVTD EEQTNVPYIY AIGDILEGKL ELTPVAIQAG
       360        370        380        390        400
RLLAQRLYGG STVKCDYDNV PTTVFTPLEY GCCGLSEEKA VEKFGEENIE
       410        420        430        440        450
VYHSFFWPLE WTVPSRDNNK CYAKVICNLK DNERVVGFHV LGPNAGEVTQ
       460        470        480        490
GFAAALKCGL TKQQLDSTIG IHPVCAEIFT TLSVTKRSGG DILQSGCUG
```

Source from <http://www.uniprot.org/uniprot/O89049>

Figure 2.1: Rat Thioredoxin Reductase 1 (TrxR1) protein sequence. Protein sequence for rat TrxR1 (P089049). Active site Cys (C) and Sec (U) are underlined at C-terminus of protein. Source: www.uniprot.org

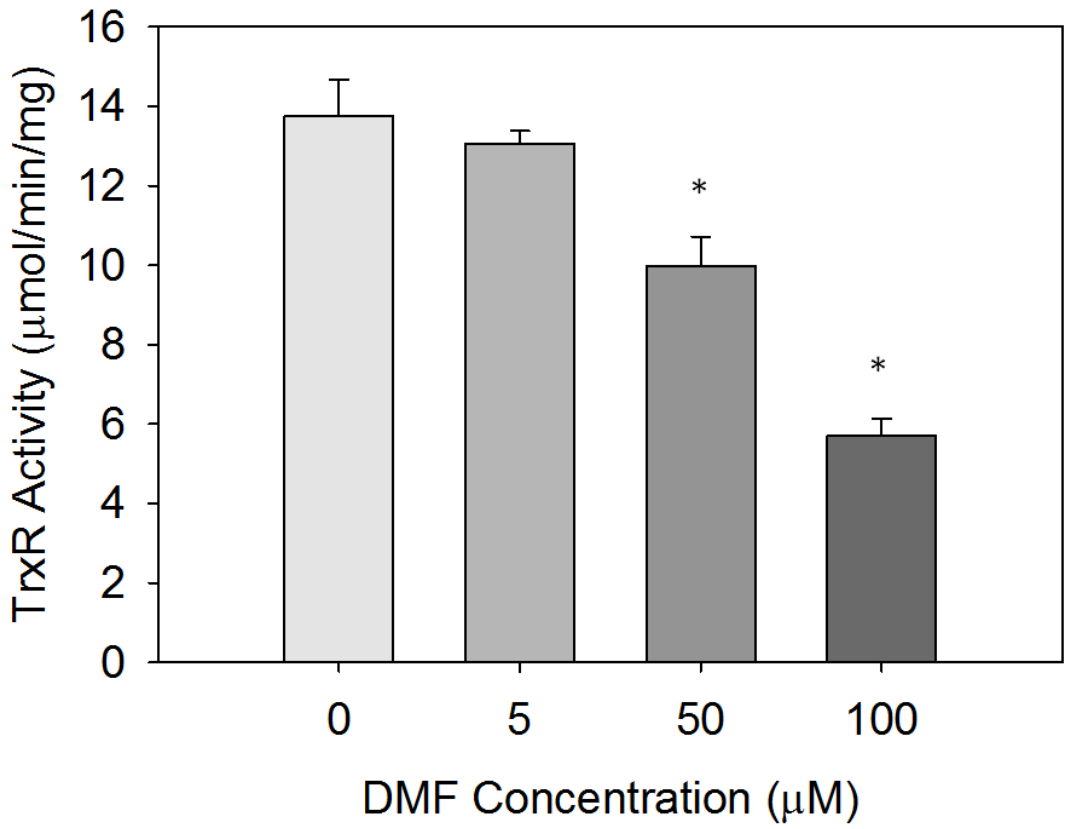

Figure 2.2: The effects of dimethyl fumarate (DMF) on TrxR activity *in vitro*. TrxR activity for rat recombinant TrxR1 protein (1.5 µg) incubated with 0, 5, 50 and 100 µM DMF for 1 hour at room temperature (n=3). Activity is expressed as the rate of molar nicotinamide adenine dinucleotide phosphate (NADPH) oxidation per mg protein (mean ± S.E.M). Statistically significant differences in enzymatic activity were found in samples incubated in 50 and 100 µM DMF compared to the control group (*P<0.001).

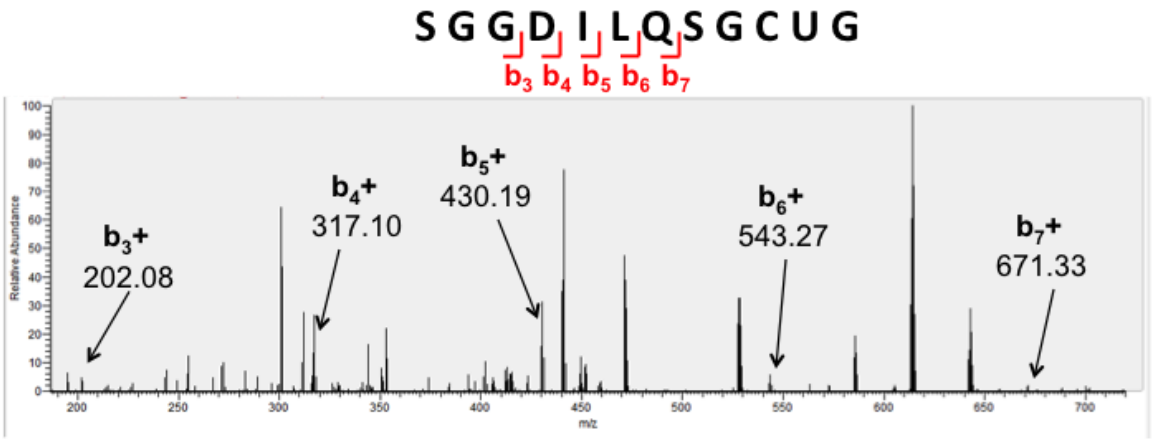

Figure 2.3: MS/MS spectrum of DMF-incubated TrxR1 terminal peptide sequence. The MMF modification was found on one of the active site residues Cys497 or Sec498. 1.5 µg purified rat recombinant TrxR1 samples were incubated in 100 µM DMF for 1 hour at room temperature and resolved by SDS-PAGE before bands were excised and digested with trypsin before high-resolution mass spectrometry (MS) analysis. The terminal peptide sequence (SGGDILQSGCUG, detected mass $[M+3H]^{+3}$=458.50 Daltons) was analyzed using MS/MS where a total of 5 fragments were identified corresponding to the MMF modification of either Cys497 or Sec498.

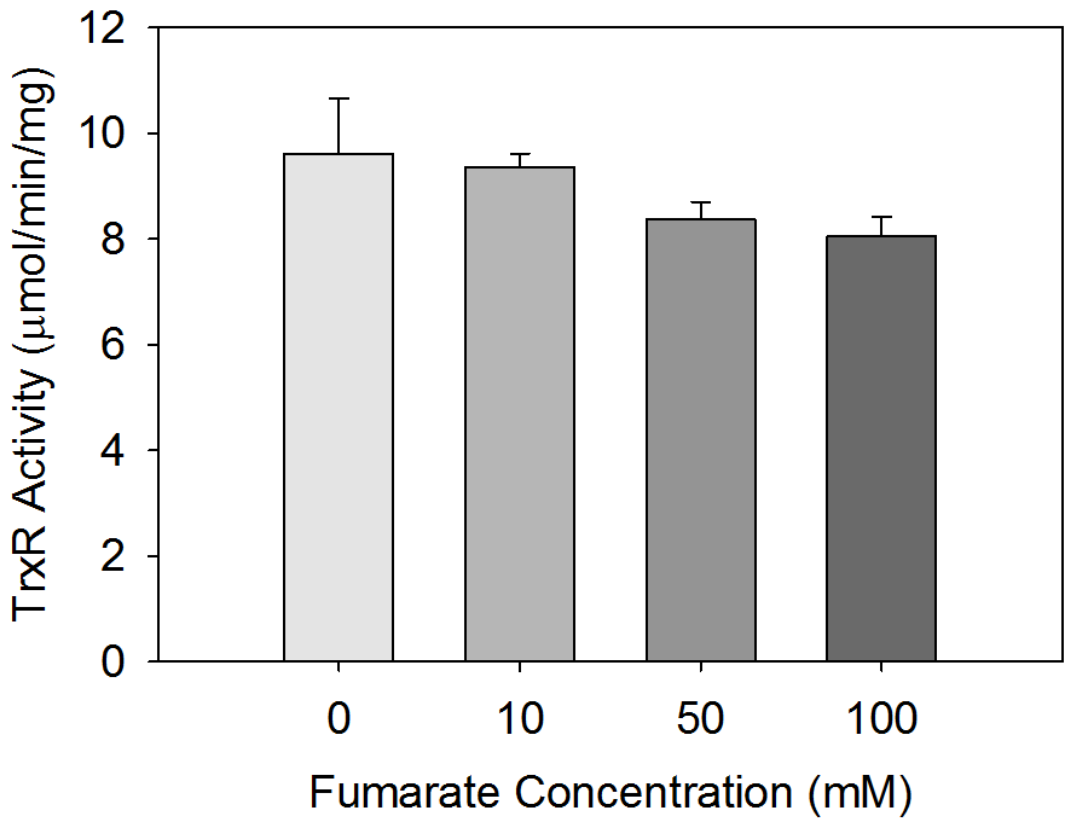

Figure 2.4: The effects of fumarate on TrxR activity *in vitro*. TrxR activity of rat recombinant TrxR1 protein (1.5 µg) incubation with 0, 10, 50 and 100 mM fumarate for 6 hours at room temperature (n=3). Activity is expressed as rate of molar nicotinamide adenine dinucleotide phosphate (NADPH) oxidation per mg protein (mean ± S.E.M). No statistically significant differences in TrxR activity were found between the groups.

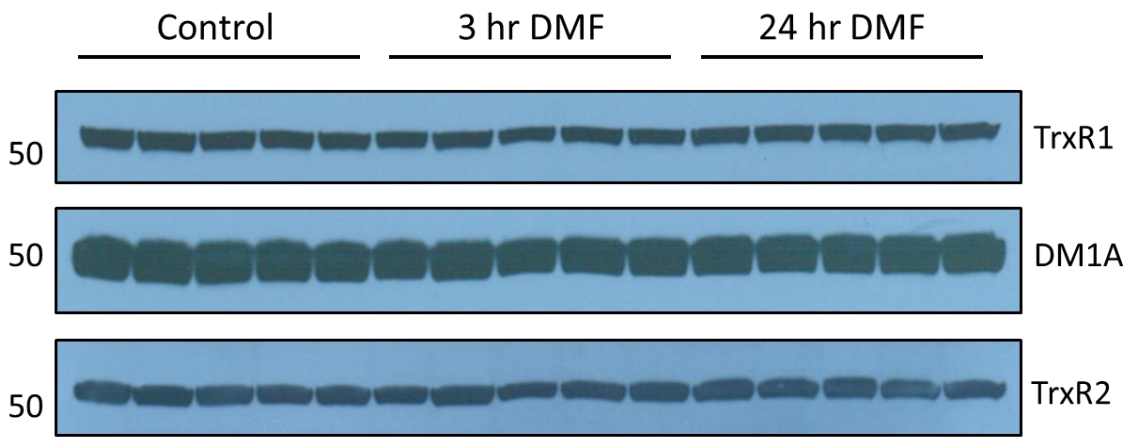

Figure 2.5: TrxR protein levels in N1E-115 cells treated with DMF. N1E-115-1 neuroblastoma cells were treated with dimethyl fumarate (DMF) either 3 hours (lanes 6-10) or 24 hours (lanes 11-15) prior to protein harvest, and compared to a control group (lanes 1-5) where no DMF was present. Western blotting was performed on the cytoplasmic lysates used to analyze protein levels of TrxR1 and TrxR2 in each group. Levels of α-tubulin (DM1A) were used to demonstrate equal protein loading. Molecular weight markers (kDa) are on the left.

Table 2.1: Mass Spectrometric data of TrxR1 peptides modified by MMF or DMF. Purified rat recombinant TrxR1 samples were incubated in 100 µM DMF for 1 hour at room temperature and resolved by SDS-PAGE before bands were excised and digested with trypsin before high-resolution mass spectrometry (MS) analysis. Initial analysis identified a total of 3 modified Cys residues; Cys177 was modified by MMF, Cys189 modified by MMF and DMF, and Cys modified by MMF. Further MS/MS analysis of the terminal peptide sequence (SGGDILQSGCUG) revealed the MMF modification on one active site residue, either Cys497 or Sec498. C^{PE}=pyridyl ethylated cysteine, PSM=peptide spectral matches (indicating the number of times the peptide was detected).

Peptide Sequence	Swiss Prot #	Monoisotopic Mass (Da)	Modification Sites	PSMs
YLGIPGDKEYC^{MMF}ISSDDLFSLPYC^{PE}PGK	089049;Q5U344	3115.43	C177	5
YLGIPGDKEYC^{PE}ISSDDLFSLPYC^{MMF}PGK	089049;Q5U344	3115.43	C189	5
YLGIPGDKEYC^{PE}ISSDDLFSLPYC^{DMF}PGK	089049;Q5U344	3129.44	C189	5
QQLDSTIGIHPVC^{DMF}AEIFTTLSVTK	089049;Q5U344	2745.40	C475	2
SGGDILQSG$C^{PE}U^{MMF}$G	-	1373.47	U498	-
SGGDILQSG$C^{MMF}U^{PE}$G	-	1373.47	C497	-

CHAPTER 3

THE EFFECTS OF ELEVATED FUMARATE LEVELS ON THIOREDOXIN REDUCTASE

3.1 Introduction

As described in Chapter 1, thioredoxin reductase (TrxR) contains Cys and Sec residues in the active site that interchange between a selenenylsulfide and selenolthiol motif during the catalytic cycles of this enzyme. TrxR is critical for the reduction of the thioredoxins (Trx) and the modulation of cellular oxidant status; therefore any compounds that inhibit TrxR are likely to perturb its reductive functions. The modification of TrxR has previously been demonstrated *in vitro* by the electrophiles 4-hydroxy-2-nonenal (a product of lipid peroxidation) and curcumin (the active component of the herb tumeric), where the Sec and other Cys residues were irreversibly alkylated causing diminished enzymatic activity (45, 46). Other TrxR inhibitors include electrophiles such as gold, platinum or other metal-containing compounds that are considered highly potent due to their high affinity for sulfur atoms (76, 77). Several electrophilic compounds containing sulfur, selenium or tellurium have also been described as either competitive or non-competitive inhibitors of TrxR or its substrates such as Trx or 5,5'-dithio-*bis*(2-dinitrobenzoic acid) (DTNB) (77, 78, 79). Recently, the inhibition of TrxR by other exogenous species such as alantolactone (the active component of the herb *Inula helenium*) and sodium arsenite ($NaAsO_2$) has been linked to

oxidative stress-mediated apoptosis in HeLa cells and pancreatic β-cells respectively (80, 81).

Most of the TrxR inhibitors previously identified are exogenous electrophilic compounds. However, prostaglandins, hormone-like compounds that are involved in inflammation, and α,β-unsaturated ketones/aldehyde products of lipid peroxidation, such as 4-hydroxy-2-nonenal, represent the few endogenously produced inhibitors of TrxR that have been studied to date. In this thesis, I investigated if TrxR was inhibited by the endogenous metabolite fumarate, during conditions where fumarate levels are elevated. In particular I was interested in adipocytes matured in high glucose, since we have previously demonstrated that succination is increased under these conditions (12, 13, 82). We have also demonstrated that adipocytes in high glucose versus normal glucose conditions have increased levels of oxidants such as hydrogen peroxide (unpublished observations). Since protein succination by fumarate is non-enzymatic and irreversible, this finding might identify a new endogenous inhibitor of TrxR that may in part explain the susceptibility of some cells to increasing oxidative stress.

3.2 Results

A 3T3-L1 mouse model was used to mimic fumarate-rich diabetic conditions where adipocytes were matured in either 5 mM or 25 mM glucose medium. Protein was harvested from the cells after 8 days of maturation, the cytoplasmic fraction was collected and special caution was taken to ensure that lipid from these cell lysates was removed following centrifugation. TrxR activity was measured in the cytoplasmic fractions of adipocyte lysates using the DTNB-reduction assay, as described in Chapter 2. The TrxR

activity is calculated through the use of a TrxR-specific inhibitor, sodium aurothiomalate (ATM). The total cellular thiol-reducing activity (samples without inhibitor present) is measured in parallel with the non-TrxR thiol reducing activity (samples containing TrxR inhibitor). TrxR activity can be calculated by subtracting the non-TrxR activity (inhibitor present) from the total thiol-reducing activity (inhibitor not present) and is expressed as the rate of molar nicotinamide adenine dinucleotide phosphate (NADPH) oxidation per mg protein (mean ± S.E.M). The 5 mM adipocyte group contained 3 out of 5 total samples that abnormally displayed higher enzymatic activities when the TrxR inhibitor was present, leaving TrxR activity unable to be calculated for these 3 samples. Unexpectedly, the average activity measured for the 5 mM adipocytes (n=2) and 25 mM adipocytes (n=5) were 1.19 ± 0.16 and 3.56 ± 0.41 nmol/min/mg, respectively (Figure 3.1). These results represent statistically different values (*$P<0.05$), where adipocytes cultured in high glucose medium (25 mM) display a ~3-fold increase in TrxR activity compared to adipocytes cultured in normal glucose (5 mM).

Levels of protein succination were analyzed using immunoblotting with an anti-2SC antibody and increases in total succinated proteins for 25 mM adipocytes in comparison to 5 mM adipocytes were confirmed (Figure 3.2, 2SC panel, lanes 6-10 vs. lanes 1-5). TrxR1 protein levels in these adipocytes were analyzed by immunoblotting to correlate the measured activities of this enzyme to its abundance in each group, however no significant differences in band intensities were observed (Figure 3.2, TrxR1 panel). Levels of α-tubulin (DM1A) were also analyzed using western blotting to demonstrate equal amounts of protein loading per well (Figure 3.2, DM1A panel).

In order to produce conditions with enhanced fumarate accumulation, a cell model was used where 3T3-L1 mouse fibroblasts were transduced with a lentivirus containing fumarase (Fh) shRNA to induce *Fh* knockdown (*Fh* k/d). These were compared to a control group transduced with a scrambled lentivirus (i.e. fumarase was not knocked-down). In order to ensure that the cells had sufficient incorporation of the virus, the plasmid also contained a puromycin resistance gene and only puromycin resistant cells were selected for further propagation. Once these cells were confluent for 7 days they were harvested and the cytoplasmic protein was collected for analysis. TrxR activity was measured in the cytoplasmic fractions of cell lysates using the same DTNB-reduction assay previously described, and the data obtained was expressed as the rate of molar NADPH oxidation per mg protein (mean ± S.E.M). The scrambled group contained 1 sample that exhibited higher activity when the TrxR-inhibitor (ATM) was present, therefore TrxR activity could not be calculated for this single instance. The average activity measured for the scrambled samples (n=4) and the *Fh* k/d samples (n=5) were 1.99 ± 0.89 and 3.05 ± 0.71 nmol/min/mg, respectively (Figure 3.3). The trend for an increase in activity in the Fh k/d cells was unexpected, however, no statistically significant differences in TrxR activity were found between the two groups.

In order to confirm that *Fh* k/d was successful in generating increased succination in these cells, SDS-PAGE coupled with immunoblotting using a polyclonal anti-2SC antibody was performed. The immunoblot revealed significant increases in total succinated proteins for *Fh* k/d samples in comparison to the scrambled group (Figure 3.4, 2SC panel, lanes 6-10 vs. lanes 1-5). The immunoblot was stripped and additional blotting was also performed to detect levels of fumarase in both groups, confirming that

Fh k/d cells had significantly less levels of this protein (Figure 3.4, Fumarase panel). TrxR1 levels, the cytoplasmic isoform of the enzyme, were also analyzed by western blotting to detect any differences in the levels of the protein between these groups, however there were no significant differences in TrxR1 (Figure 3.4, TrxR1 panel). Finally, the levels of α-tubulin (DM1A) were assessed as a loading control to demonstrate equal amounts of protein loading per well (Figure 3.4, DM1A panel).

3.3 Discussion

The thioredoxin system, composed of Trx, TrxR and NADPH, is a ubiquitous disulfide reducing system involved in redox regulation for various cellular processes (39, 40, 83). TrxR is a selenoprotein with high reducing capabilities due to the reactive penultimate Sec residue in the active site of the enzyme. The two major isoforms of the TrxR include the cytoplasmic TrxR1 and the mitochondrial TrxR2. The exposed position and the high reactivity of the Sec residue in TrxR allow the enzyme to be readily modified by both endogenous and exogenous electrophiles, resulting in decreased enzymatic activity (45, 46, 77). In Chapter 2 of this thesis I identified a novel TrxR inhibitor, dimethylfumarate (DMF), which inhibits enzymatic activity due to the succination of several Cys containing peptides, including the active site (Figure 2.2).

The results of the *in vitro* experiments with recombinant TrxR1 and DMF served as a positive control and provided evidence that TrxR could be succinated leading to reduced enzymatic activity. The next aim of this thesis was to determine if TrxR is susceptible to succination by elevated levels of fumarate in cellular models. If present, this modification of TrxR would identify a new endogenous TrxR-inhibiting metabolite

that is present at elevated levels during certain disease conditions. Hereditary leiomyomatosis and renal cell cancer (HLRCC) leads to an accumulation of fumarate due to mutations or deficiencies in the enzyme fumarase, responsible for converting fumarate to malate (15). In the adipocyte, increased cellular metabolism due to elevated extracellular glucose concentrations, such as in diabetic conditions, will lead to an increase in ATP/ADP ratios and an accumulation of ATP. This accumulation inhibits the mitochondrial electron transport chain through respiratory control, and increasing the mitochondrial membrane potential ($\Delta\psi_m$) and $NADH/NAD^+$ ratio, leading to an accumulation of fumarate (13) (Figure 1.2). The cell models utilized in the described studies sought to mimic each of these disease conditions in order to study the effects of elevated fumarate on TrxR and its activity.

In the adipocyte model, western blotting revealed that increases in levels of total protein succination in cells grown in high glucose (25 mM) (Figure 3.2, 2SC panel), however, the levels of TrxR1 were unchanged (Figure 3.2, TrxR1 panel). TrxR activity in cells matured in 25 mM glucose (n=5) had significantly higher activity compared to those matured in 5 mM glucose (n=2) (Figure 3.1). It is worth noting that the 5 mM group contained 3 samples in which TrxR activity could not be measured due to issues with the activity assay. As mentioned in the results, the assay requires the use of a TrxR-specific inhibitor (sodium aurothiomalate) that allows TrxR activity to be calculated by subtracting the non-TrxR thiol-reduction activity from the total thiol-reduction activity. The 3 samples that were excluded from the reported TrxR activity (Figure 3.1) exhibited higher activities when the TrxR-inhibitor was present in comparison to the total activity (no inhibitor present), meaning TrxR activity could not be reliably calculated. In contrast

to the fibroblast cell model where TrxR1 protein levels and activity were not different between the two groups, an accurate explanation for the increase in TrxR activity for 25 mM adipocytes is less clear. Keap1 succination by elevated fumarate levels and the subsequent activation of the Nrf2 pathway could explain an increase in the 25 mM TrxR activity due to the presence of more of this protein, however protein levels remain the same as in the 5 mM group (Figure 3.2, TrxR1 panel). While it is unfortunate that we cannot fully conclude if TrxR is endogenously succinated in adipocytes *in vitro*, these results suggest that it may not be. In the future, we hope to further examine the effects of enhanced fumarate conditions on TrxR in cellular models while utilizing a different TrxR activity assay.

Despite the large increase in succinated proteins in the *Fh* k/d fibroblasts, there was no significant decrease in total TrxR activity when compared to scrambled controls, in fact the data showed a trend towards increased TrxR activity in the *Fh* k/d cells (Figure 3.3). This led us to hypothesize that the cells may be compensating for the fumarate mediated insult by increasing the levels of antioxidant proteins such as TrxR1. However Western blotting revealed that protein levels of TrxR1 in these fibroblasts did not show any apparent changes in the fumarase-deficient cells (Figure 3.4, TrxR1 panel). Levels of the mitochondrial TrxR2 were not analyzed since the lysates used in the activity assays are cytoplasmic fractions and should contain limited mitochondrial proteins. Considering the lack of inhibition of enzymatic TrxR activity, as well as the equal levels of TrxR1 protein between the scrambled and *Fh* k/d cells, it is appears that TrxR was not modified by fumarate as originally predicted. Fumarate is not as reactive as DMF, and perhaps it is unable to compete with the endogenous TrxR substrates, such as Trx, and induce

succination. It is also possible that elevated fumarate levels in *Fh* k/d fibroblasts lead to the succination of TrxR1 and the protein was rapidly turned-over. Elevated levels of fumarate are also known to cause succination of Kelch-like ECH-associated protein-1 (Keap1) that, under normal circumstances, interacts with the transcription factor nuclear factor (erythroid-derived 2)-like-2 (Nrf2), preventing its translocation to the nucleus and promoting transcription of target genes (2, 7, 82). Succinated Keap-1 results in its dissociation with Nrf2, allowing Nrf2 to promote the transcription of various cytoprotective and antioxidant enzymes, including TrxR1 (84, 85, 86). Degradation of succinated TrxR1 and the expression of additional protein in *Fh* k/d cells after Nrf2 activation could explain the relatively equal amount of TrxR activity and TrxR1 protein levels compared to the control samples. The assessment of TrxR activity over several hours, or in the presence of cycloheximide to prevent translation of new protein, may be required to determine if a relatively equal rate of synthesis:degradation contributed to the results observed.

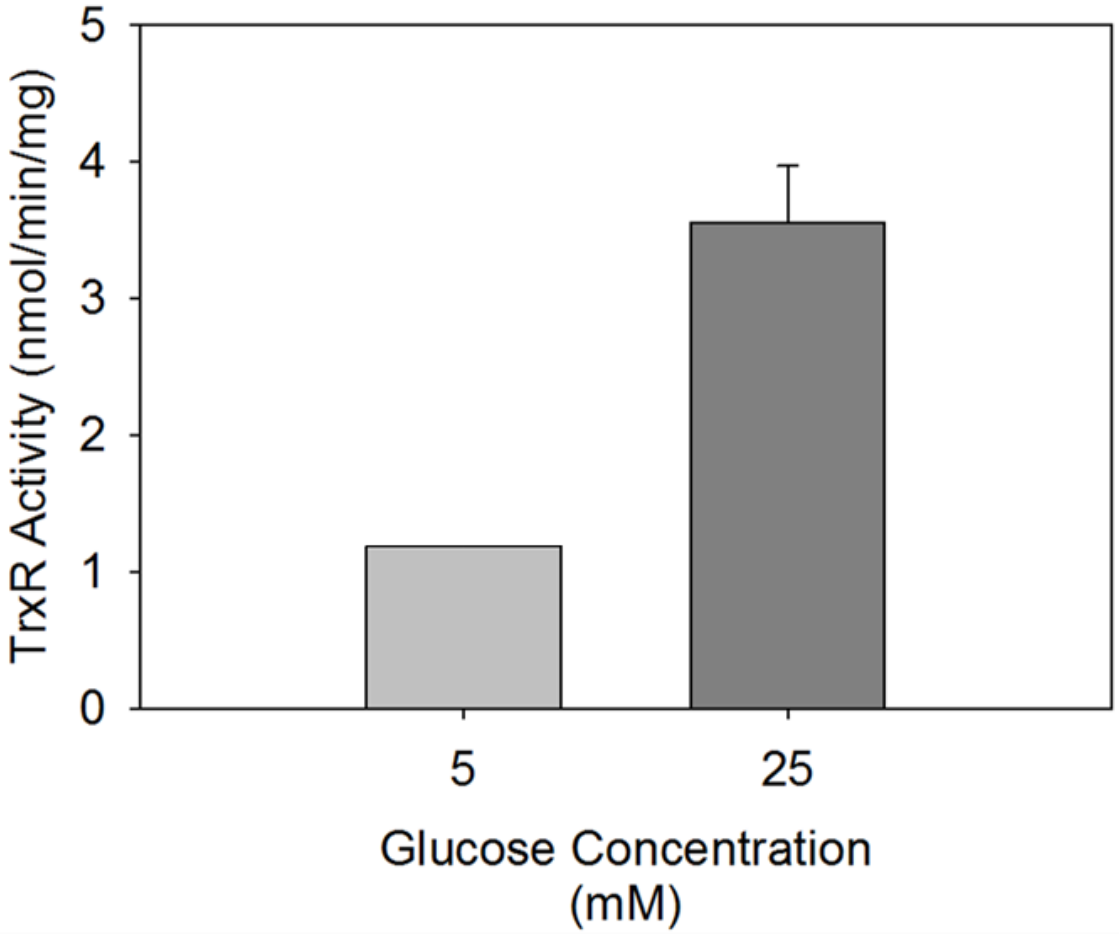

Figure 3.1: TrxR activity in 5 mM vs 25 mM 3T3-L1 adipocytes. 3T3-L1 adipocytes were matured in 5 mM or 25 mM glucose for 8 days. Cellular thioredoxin reductase (TrxR) activity was measured in lysates using a DTNB reduction assay and expressed as the molar rate of nicotinamide adenine dinucleotide phosphate (NADPH) oxidation per mg protein (5 mM glucose n=2, mean ± S.E.M.; 25 mM glucose n=5, mean ± S.E.M.). Significant differences were found between 5 mM and 25 mM groups (*$P < 0.05$) with the 25 mM group showing a ~3 fold increase in TrxR activity.

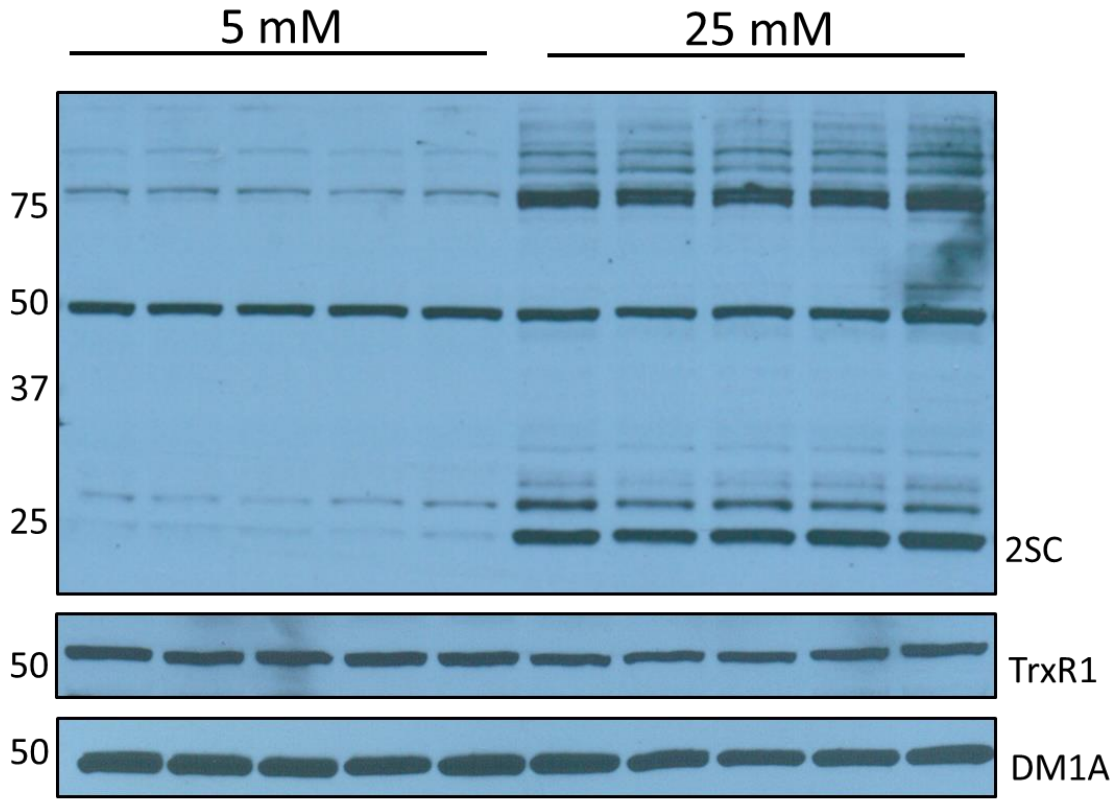

Figure 3.2: Western blot of TrxR levels in 5 mM vs 25 mM 3T3-L1 adipocytes. 3T3-L1 adipocytes were matured in 5 mM (lanes 1-5) or 25 mM (lanes 6-10) glucose for 8 days. Protein (30 µg) was separated using 1-D SDS-PAGE and detection of 2SC was performed using a polyclonal anti-2SC antibody. Western blotting was also used to analyze protein levels of TrxR1 to determine if differences existed between the two groups. The levels of α-tubulin (DM1A) were determined to sure equal protein loading. MW markers are shown in kDa on the left.

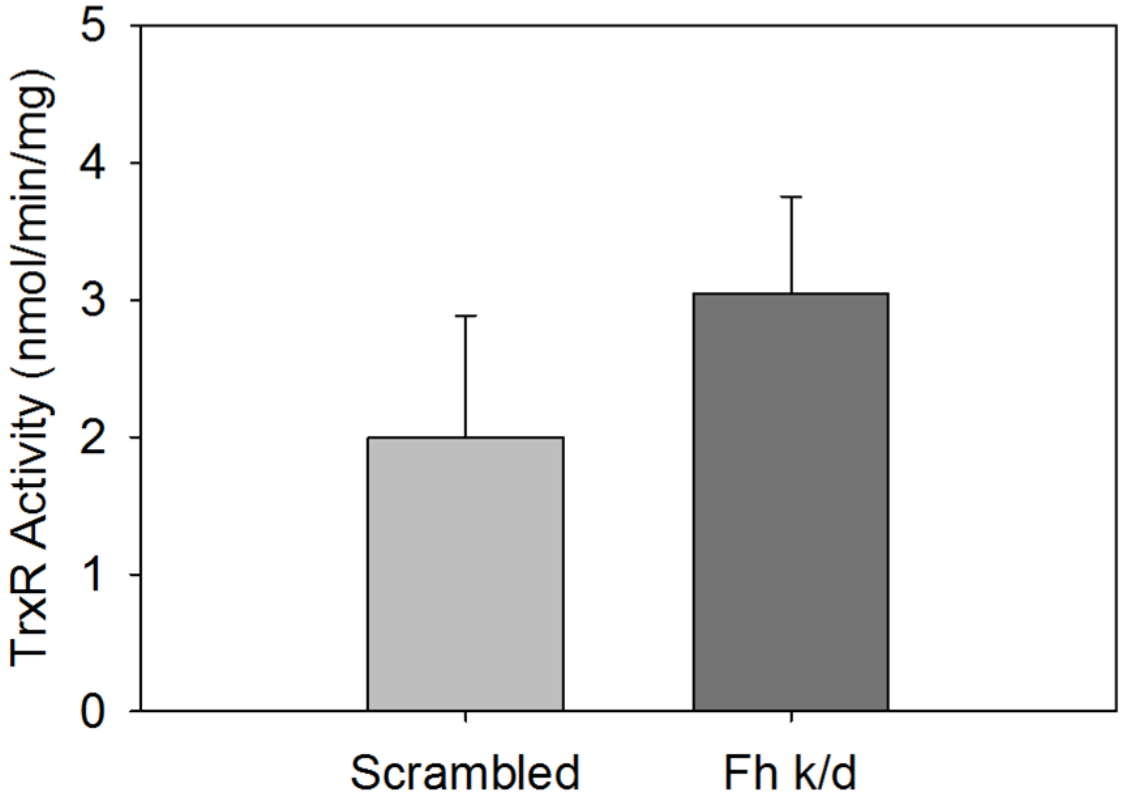

Figure 3.3: TrxR activity in Scrambled vs. *Fh* k/d 3T3-L1 fibroblasts. 3T3-L1 fibroblasts were transfected with a scrambled lentivirus or a lentivirus containing an shRNA that knocks down fumarase (Fh). Cellular thioredoxin reductase (TrxR) activity was measured in lysates using a DTNB reduction assay and expressed as the molar rate of nicotinamide adenine dinucleotide phosphate (NADPH) oxidation per mg protein (scrambled n=4, mean ± S.E.M.; *Fh* k/d n=5, mean ± S.E.M.). No significant differences between scrambled and *Fh* k/d groups.

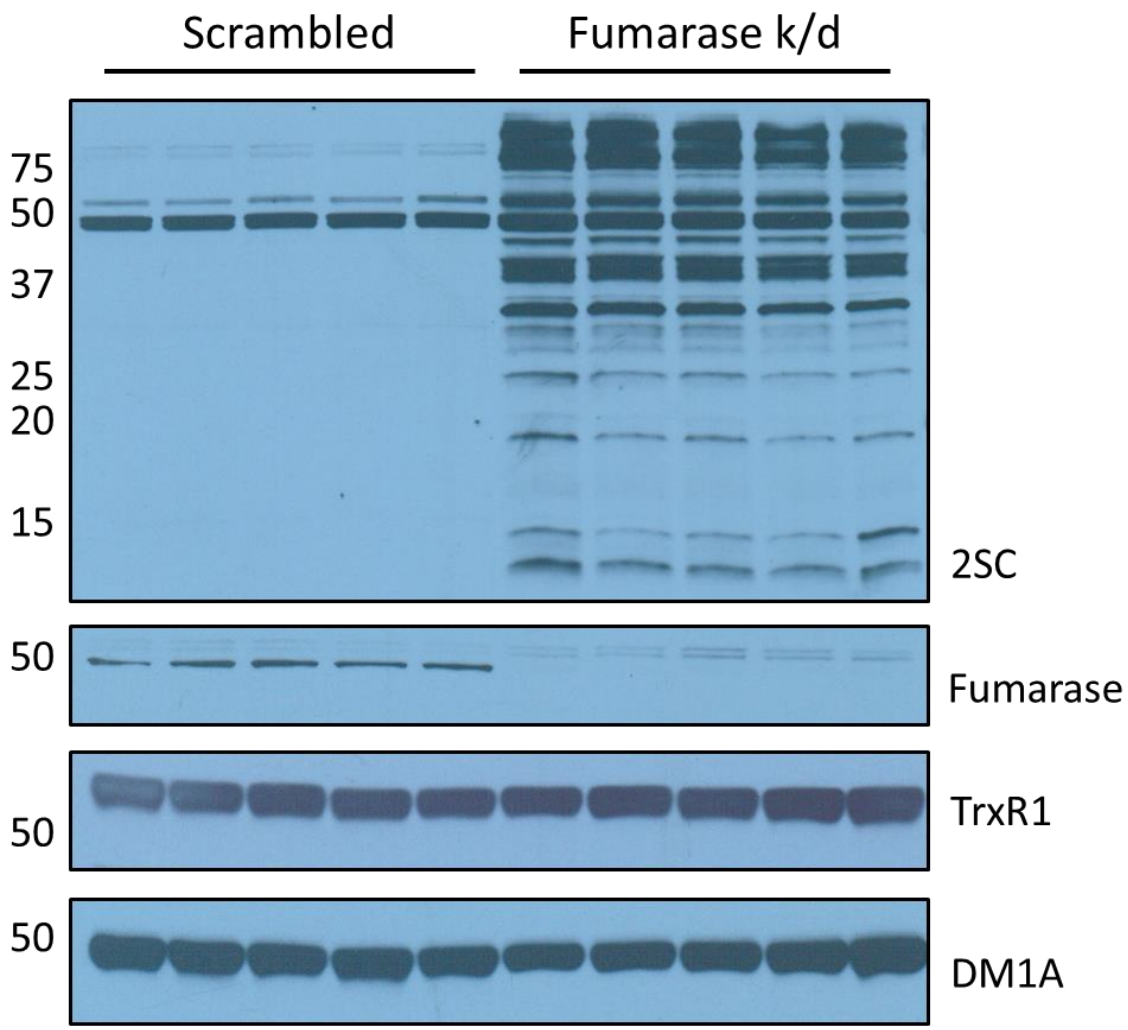

Figure 3.4: Western blot of TrxR levels in scrambled vs *Fh* k/d 3T3-L1 fibroblasts. 3T3-L1 fibroblasts were transfected with a scrambled virus (lanes 1-5) or viral shRNA that knocks down fumarase (Fh) (lanes 6-10). Protein (30 µg) was separated using 1-D SDS-PAGE and detection of 2SC was performed using a polyclonal anti-2SC antibody. Western blotting was also used to analyze protein levels of TrxR1 to determine if differences existed between the two groups, and to analyze levels of fumarase to confirm the knockdown in *Fh* k/d cells. MW markers are shown in kDa on the left and α-tubulin (DM1A) was used as a loading control.

CHAPTER 4

THE EFFECTS OF FUMARATE AND DIMETHYL FUMARATE (DMF) ON GLUTATHIONE PEROXIDASE

4.1 Introduction

Glutathione peroxidase (GPx) is a highly conserved selenoenzyme that contributes significant protective functions as a scavenger of damaging reactive oxygen species (ROS) in the cell. Due to its essential role, identifying compounds that may impede its normal function would prove to be very beneficial in understanding how ROS imbalance occurs during disease states. In contrast to thioredoxin reductase (TrxR), there are fewer inhibitors of GPx described in the literature, and the detailed mechanisms of inhibition for most of those identified are not completely understood. Recently, proteomic analysis has identified the succination of Cys202 of GPx1 in a fumarase (Fh) deficient tumor, where levels of fumarate are enhanced due to a mutation of the Kreb's cycle enzyme responsible for converting fumarate to malate (16). Although the effects of this modification on GPx activity were not investigated, this result established that this enzyme could be modified by fumarate intracellularly. Although Cys202 is not in the active site of GPx, its ability to be succinated, and the presence of an additional Sec in this enzyme's active site, provided a reason for this thesis to examine GPx activity in similar models where fumarate is enhanced.

Coenzyme A, an acyl carrier involved in the synthesis and oxidation of fatty acids and the oxidation of pyruvate, has also been described as a GPx inhibitor at low concentrations, however its mechanism of interaction with GPx is largely unknown (87). 4-hydroxy-nonenal (HNE), an aldehyde produced during lipid peroxidation and a previously described TrxR inhibitor (46), has been demonstrated to cause concentration-dependant inhibition of bovine erythrocyte GPx, which was hypothesized to be the caused by the modification of non-specific Cys residues (88). The exact mechanism was not identified, however in experiments where GPx was pre-incubated with thiols such as glutathione (GSH), the inhibition by HNE was not observed; proposed to be blocked by GSH binding to GPx (88).

More specifically, the oxidation and subsequent inactivation of GPx has been described in greater detail using both endogenous and exogenous pro-oxidants. S-nitroso-N-acetyl-D,L-penicillamine (SNAP) is an exogenous precursor to the vasodilator nitric oxide (NO) and causes the oxidation of Sec and Cys residues on GPx, resulting in the formation of either disulfide (Cys-Cys) or selenyl sulfide (Sec-Cys) bonds that cause inhibition of the enzyme, presumably inhibiting the catalytic cycle (89). More potent oxidants such as peroxynitrite, a strong nucelophilic product of nitric oxide (NO) reacting with superoxide (O_2^-), and 3-morpholinosydnonimine-N-ethylcarbamide, a precursor to the oxidant, peroxynitrite, also caused dose-dependent inhibition of GPx through oxidative modification of thiols or selenols (89, 90). Currently, oxidative modification represents the most characterized type of GPx inhibition; however this thesis aims to determine if irreversible succination by endogenously produced fumarate is also capable of inhibiting GPx in cell culture systems.

4.2 Results

In order to test the ability to modify GPx and alter its activity *in vitro*, experiments were conducted using bovine erythrocyte glutathione peroxidase (GPx, predominantly GPx1). The protein was incubated in 0, 10, 25, 50 and 100 µM dimethylfumarate (DMF, a reactive fumarate ester that we considered a positive control) for 1 hour at room temperature. GPx activity was measured and expressed as the molar rate of nicotinamide adenine dinucleotide phosphate (NADPH) oxidation per mL (mean ± S.E.M., Figure 4.1). Statistically significant differences in GPx activity could not be detected, even with elevated concentrations of DMF. A similar experiment was performed where bovine erythrocyte GPx was incubated in 0, 5, 10, 15, 25 and 50 mM fumarate for 6 hours at room temperature. GPx activity was measured and expressed as the molar rate of NADPH oxidation per mL (mean ± S.E.M., Figure 4.2). However no statistically significant differences in GPx activity could be detected. Several additional experiments were performed where the protein was treated with either DMF or fumarate for varying incubation times and temperatures, however no consistent reduction in activity was detected (data not shown).

In order to mimic diabetic conditions, a cell model was used where 3T3-L1 mouse adipocytes were matured in either 5 mM or 25 mM glucose medium. GPx activity was measured in the cytoplasmic fractions of cell lysates and expressed as the rate of molar NADPH oxidation per mg protein (mean ± S.E.M). The average activity measured for the 5 mM adipocytes (n=5) and 25 mM adipocytes (n=5) were 10.60 ± 0.64 and 7.91 ± 0.73 nmol/min/mg, respectively (Figure 4.3). These results represent statistically different values (*$P<0.05$), where adipocytes cultured in high glucose medium (25 mM) display an

average ~25% decrease in GPx activity compared to adipocytes cultured in normal glucose (5 mM). These results suggested that GPx activity was reduced in high glucose specifically, potentially as a result of succination.

SDS-PAGE followed by immunoblotting was performed to analyze the differences in total succinated proteins in adipocytes matured in 5 mM vs 25 mM glucose (Figure 4.4, 2SC panel, lanes 1-5 vs. lanes 6-10). Western blotting was also performed to analyze protein levels of the two most abundant GPx isoforms, GPx1 and GPx4, and to correlate these levels to enzymatic activity data. There were no obvious differences in protein levels of either GPx1 (Figure 4.4, GPx1 panel) or GPx4 (Figure 4.4, GPx4 panel) for adipocytes matured in 5 mM vs. 25 mM glucose. Protein levels of α-tubulin (DM1A) were also analyzed using western blotting and used as a loading control (Figure 4.4, DM1A panel). Densitometry was performed on the immunoblots to determine the relative ratio of intensity of GPx1 (Figure 4.5) and GPx4 (Figure 4.6) bands normalized to DM1A band intensity for 5 mM or 25 mM sample, confirming that no significant differences in either of these proteins between the groups could be established.

An additional cell culture model was used to examine the effects of enhanced fumarate accumulation on intracellular GPx; the same fibroblast model was used as for the TrxR experiments (see Chapter 3). 3T3-L1 mouse fibroblasts were transduced with fumarase knock-down (*Fh* k/d) lentiviral shRNA and compared to a control group containing a scrambled lentivirus (i.e. fumarase was not knocked-down). The virus also contained a puromycin resistance gene in the plasmid to ensure the selection of only the cells transduced with the virus. After 7 days of confluency, cellular protein was harvested and the cytoplasmic fractions were collected for analysis. GPx activity was measured in

the cytoplasmic fractions of cell lysates and expressed as the rate of molar NADPH oxidation per mg protein (mean ± S.E.M). The average activity measured for the scrambled samples (n=5) and the *Fh* k/d samples (n=5) were 34.25 ± 1.76 and 39.45 ± 2.31 nmol/min/mg, respectively (Figure 4.7**)**. However no statistically significant differences in GPx activity were detected between the two groups.

Increases in total protein succination were detected through immunoblotting in *Fh* k/d samples in comparison to scrambled controls (Figure 4.8, 2SC panel, lanes 6-10 vs. lanes 1-5). Decreased levels of fumarase were also detected in the *Fh* k/d group compared to the scrambled control by immunoblotting, confirming its knockdown by shRNA (Figure 4.8, Fumarase panel). Western blots were also probed for GPx1 to detect any changes in protein levels between these groups, however there were no apparent differences (Figure 4.8, GPx1 panel). Levels of α-tubulin (DM1A) were used as a loading control to demonstrate equal amounts of protein loading per well (Figure 4.8, DM1A panel).

4.3 Discussion

My original hypothesis predicted that incubations with the highly reactive DMF or the endogenous metabolite fumarate would result in decreased enzymatic activity. However, contrary to this hypothesis, consistent changes in recombinant bovine GPx activities could not be observed after incubation with either DMF or fumarate *in vitro*, despite performing several experiments in each of these models. The position of the active site Sec and its accessibility to molecules such as fumarate or DMF may be related to observed lack of modification. Molecular modeling of GPx reveals that the active site

is located at the ends of long α-helices and is surrounded by aromatic side-chains (91, 92). Sec resides in position 47 of the 201 amino acids in the bovine GPx sequence (Figure 4.9), and may not be as substrate-accessible if there are some negatively charged amino acids nearby since fumarate contains 2 carboxyl groups. Treatment of HeLa cells with the cytotoxic compounds iludin S, a natural compound produced by fungi, and acylfulvene (AF), a semi-synthetic derivative of iludin S, caused inhibition of TrxR by irreversible binding to Sec but had no effect on GPx activity (92). While GPx may not be as reactive, this study highlights the increased exposure of the TrxR active site and therefore its increased susceptibility to chemical modification in comparison to the GPx active site. However, while I intend to pursue TrxR further, my cumulative data thus far suggests that fumarate may not be sufficiently reactive with either protein active site *in vitro*.

Increases in total protein succination by immunoblotting were detected in Fh k/d fibroblasts compared to scrambled controls (Figure 4.8, 2SC panel), however no detectable decrease in GPx activity could be observed (Figure 4.7), despite the initial hypothesis of this enhanced endogenous fumarate model leading to the succination and inhibition of this selenoenzyme. The protein levels of GPx1 did not appear to change after western blotting analysis in the Fh k/d cells (Figure 4.8, GPx1 panel), consistent with the activity data. Although fumarate levels were elevated in Fh k/d cells, it is unlikely that succination occurred on the Sec residue of GPx, which would result in a decrease in enzymatic activity. In contrast, a ~25% decrease in GPx activity was detected in 3T3-L1 adipocytes matured in high glucose (25 mM) versus cells matured in normal glucose (5 mM) (Figure 4.5). In order to correlate GPx activity to the levels of this

protein, both the GPx1 and GPx4 isoforms were analyzed with western blotting. The enzymatic activity assay measures total GPx activity, where each of the isoforms contributes to the activity detected. Therefore, we were interested in determining GPx4 levels for the adipocyte model because this enzyme is responsible for protection from lipid peroxidation and we hypothesized that GPx4 is more abundant in the lipid-rich adipocyte. Western blotting and densitometric analysis revealed no significant changes in the protein levels of GPx1 or GPx4 (Figure 4.4, GPx1/GPx4 panel), suggesting that the decrease in enzymatic activity detected in 25 mM cells is attributed to the chemical modification and inhibition of GPx as opposed to decreased amounts of this enzyme.

Although a pronounced decrease in GPx activity was detected in an adipocyte model that mimics hyperglycemic conditions, and it appears it is not due to protein succination, the reason for decreased activity can only be speculated upon without further investigation. Adipocytes contain high levels of triglycerides that are subject to lipid peroxidation, a process that produces reactive aldehydes (e.g. HNE) that have been shown to covalently modify proteins (a process known as carbonylation) (93). Adipocyte proteins are among the most heavily carbonylated (93), and it is possible that this type of modification could be contributing to the observed decrease in GPx activity for adipocytes matured in high glucose. Unfortunately I was unable to successfully immunoprecipitate GPx from these samples with the antibodies available in our laboratory, however future work on this project may lead to the successful isolation of this protein for proteomic analysis and detection of possible carbonylation or succination. Regardless, we know that hyperglycemic conditions will lead to in an increase in intracellular fumarate levels as well as glucose-derived H_2O_2, creating a greater need for

antioxidants such as GPx (13, 38). Our cell model displayed a significant reduction of GPx activity in cells cultured in 25 mM glucose, and I believe these results confirm that the adipocyte GPx capability is defective during glucotoxic conditions.

Since the assay for GPx activity provided reliable data and we did not detect decreases in the Fh k/d cells (Figure 4.7), it appears that fumarate alone does not modify the activity of GPx. As mentioned earlier in this Discussion, it is possible that other factors such as negative charges surrounding the Sec in the folded protein decrease fumarate reactivity with GPx, despite the pK_a of the active site Sec. Further studies on the succination of other proteins containing low pK_a thiols versus accessible thiols may allow us to further understand the factors that govern a proteins reactivity with fumarate.

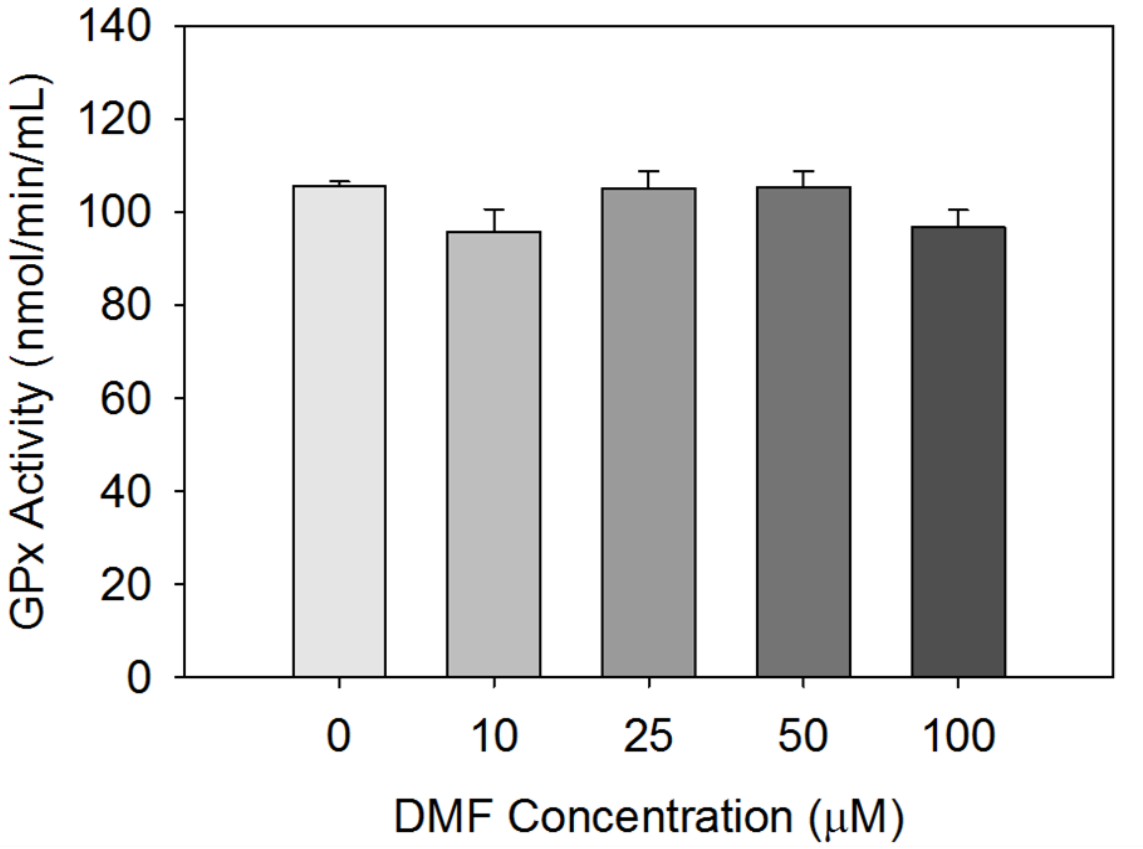

Figure 4.1: The effects of DMF on GPx activity *in vitro*. Enzymatic activity of bovine erythrocyte glutathione peroxidase (GPx) incubated with 0, 10, 25, 50 or 100 μM dimethyl fumarate (DMF) for 1 hour at room temperature (n=3). Activity is expressed as mean ± S.E.M. of the molar rate of NADPH oxidation per mL of protein. No statistically significant differences were found in GPx activity between the groups.

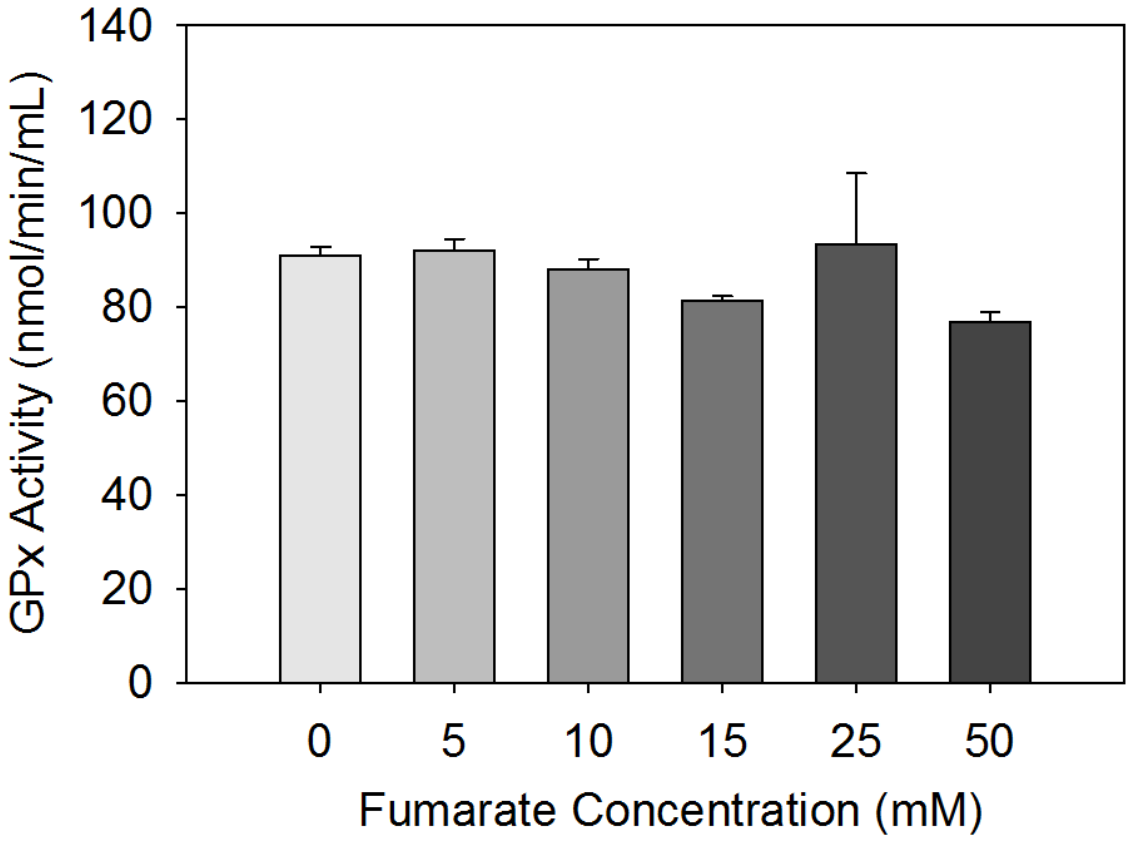

Figure 4.2: The effects of fumarate on GPx activity *in vitro*. Enzymatic activity of bovine erythrocyte GPx incubated with 0, 10, 15, 25 or 50 mM fumarate for 6 hours at room temperature. Activity is expressed as mean ± S.E.M. of the molar rate of NADPH oxidation per mL of protein (n=3). No statistically significant differences were found in GPx activity between the groups.

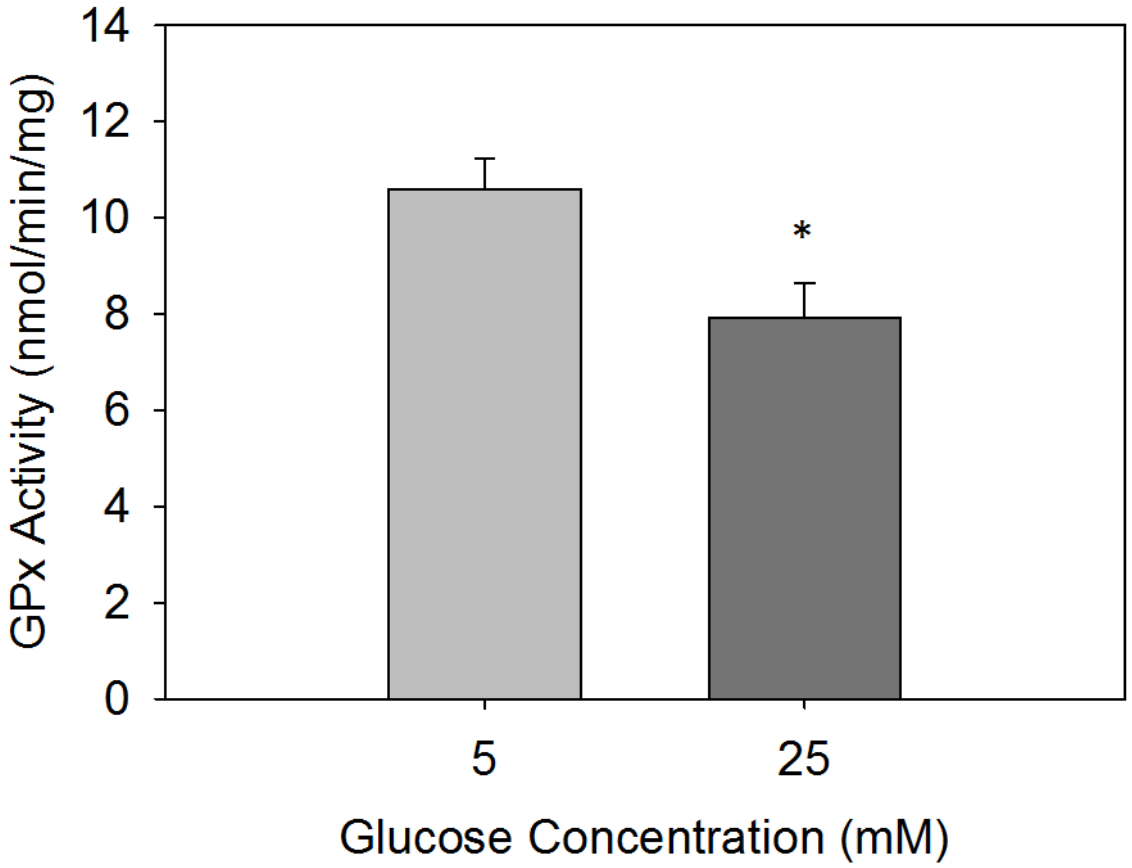

Figure 4.3: GPx activity in 5 mM vs 25 mM 3T3-L1 adipocytes. 3T3-L1 adipocytes were matured in 5 mM or 25 mM glucose for 8 days. Cellular TrxR activity was measured in lysates using colorimetric GPx activity assay that utilizes glutathione (GSH), glutathione reductase (GR) and nicotinamide adenine dinucleotide phosphate (NADPH). GPx activity is expressed as the molar rate of NADPH oxidation per mL of protein (5 mM glucose n=5, mean ± S.E.M.; 25 mM glucose n=5, mean ± S.E.M.). Significant differences were found between 5 mM and 25 mM groups (*P < 0.05) with the 25 mM group showing a ~25% decrease in GPx activity.

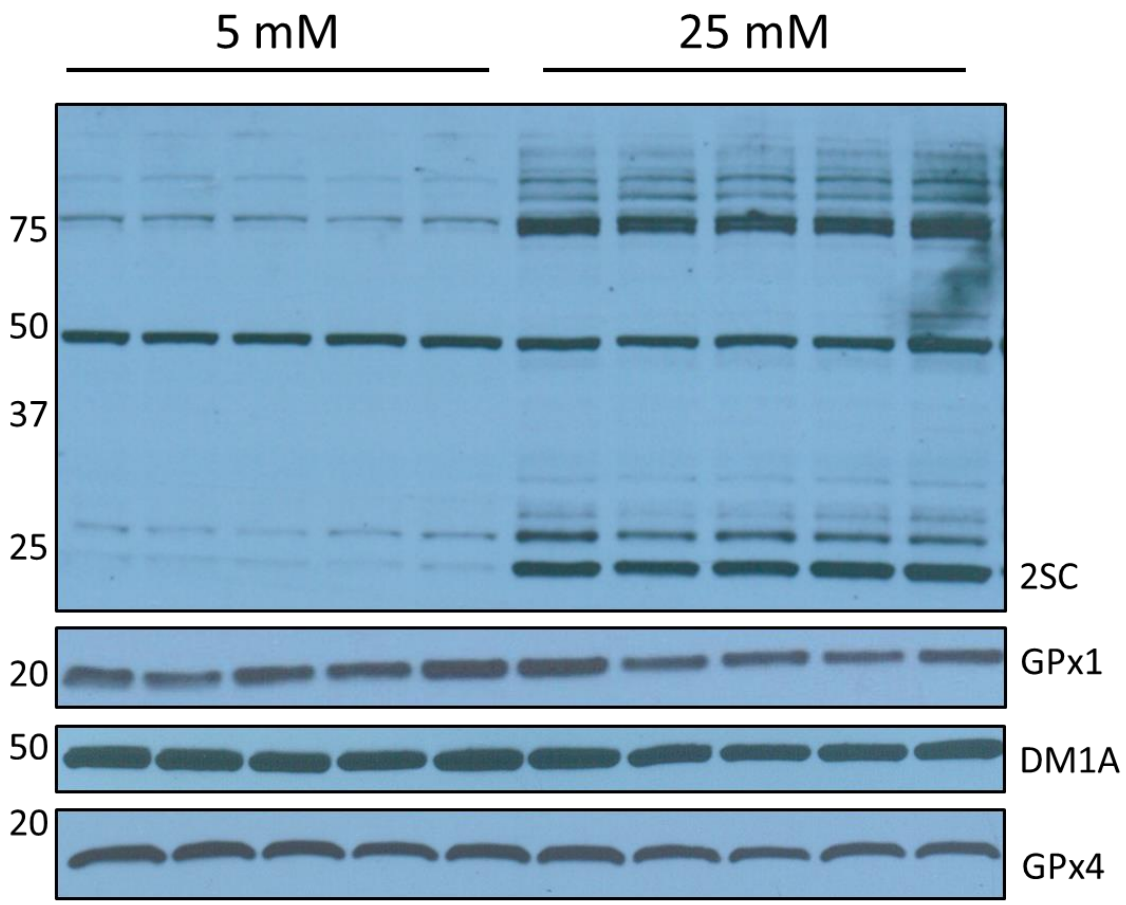

Figure 4.4: Western blot of GPx levels in 5 mM vs. 25 mM 3T3-L1 adipocytes. 3T3-L1 adipocytes were matured in 5 mM (lanes 1-5) or 25 mM (lanes 6-10) glucose for 8 days. Protein (30 µg) was separated using 1-D SDS-PAGE and detection of 2SC was performed using a polyclonal anti-2SC antibody. Western blotting was also used to analyze protein expression of GPx1 and GPx4 to determine if differences existed between the two groups using levels of α-tubulin (DM1A) as a loading control. MW markers are shown in kDa on the left.

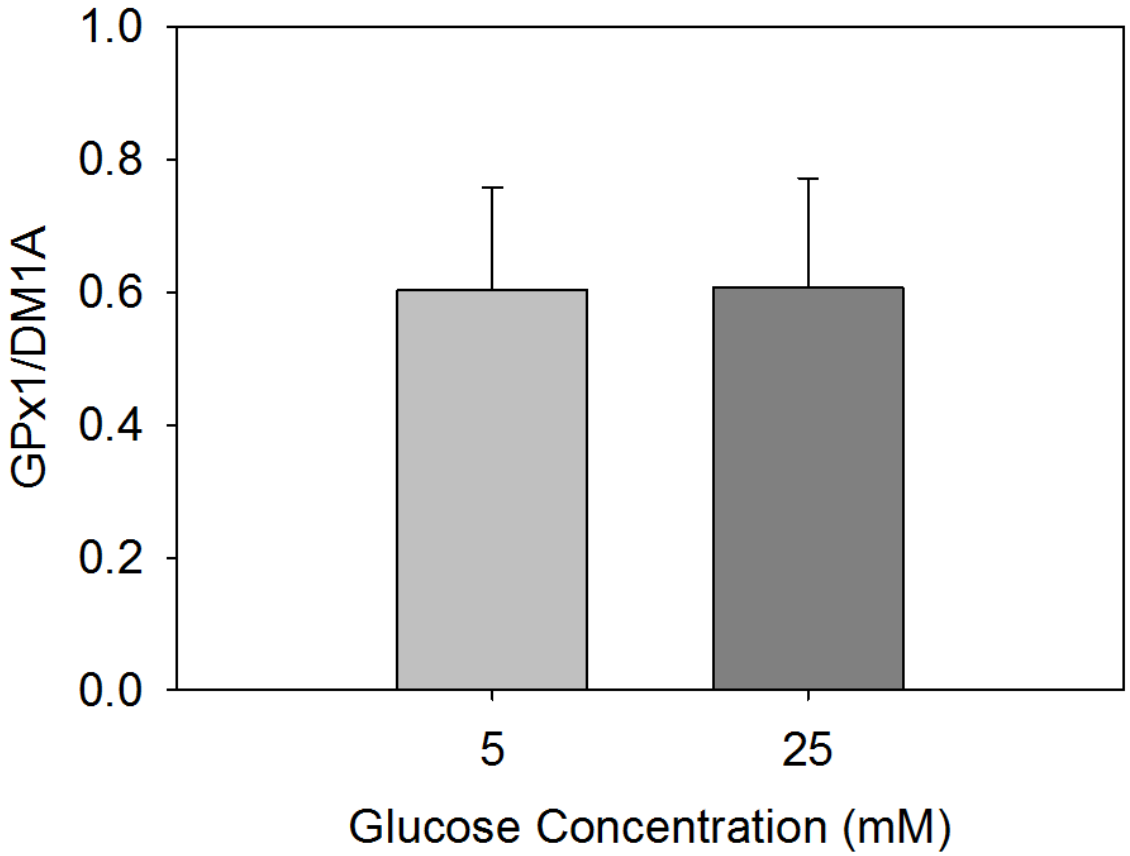

Figure 4.5: Densitometric analysis of GPx1/DM1A levels in 3T3-L1 adipocytes. Densitometric analysis of GPx1/DM1A levels from western blot of 3T3-L1 adipocytes grown in 5 mM (n=5) or 25 mM (n=5) glucose, expressed as mean ±S.E.M. No statistical significances were detected.

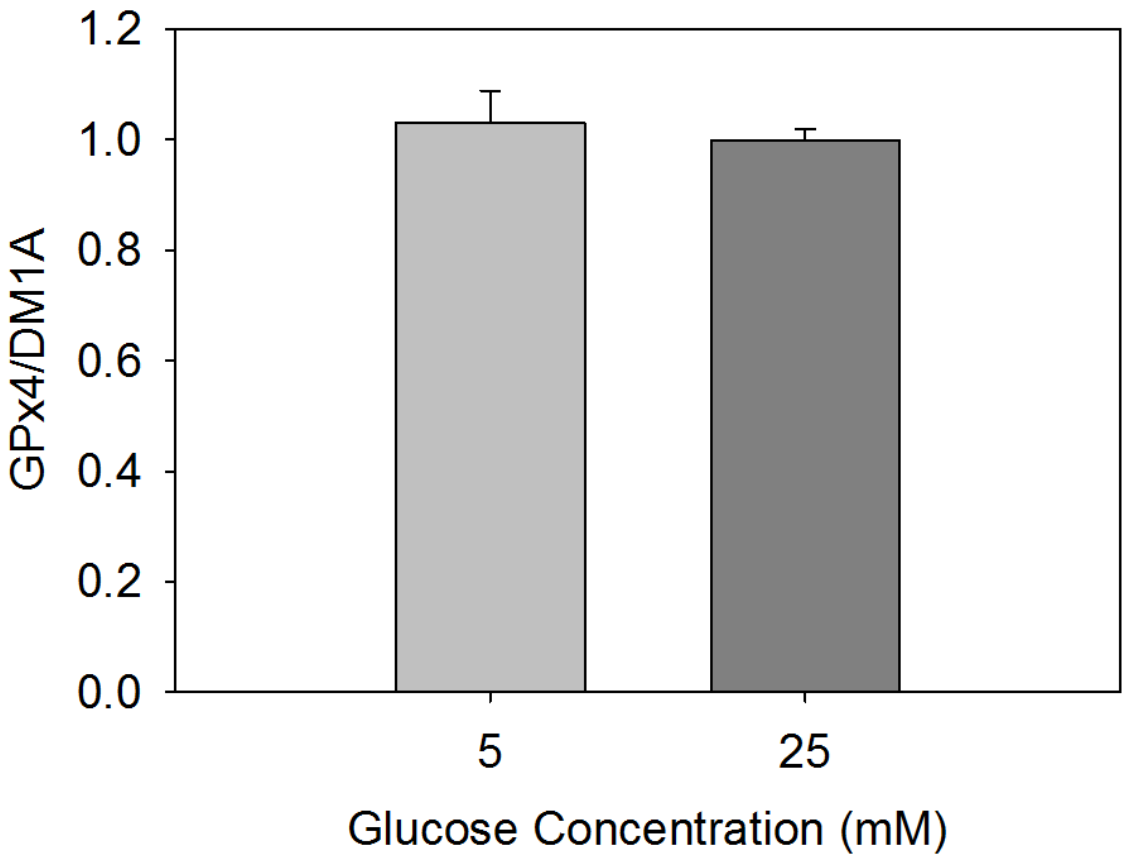

Figure 4.6: Densitometric analysis of GPx4/DM1A levels in 3T3-L1 adipocytes. Densitometric analysis of GPx4/DM1A levels from western blot of 3T3-L1 adipocytes grown in 5 mM or 25 mM glucose, expressed as mean ±S.E.M. No statistical significances were detected.

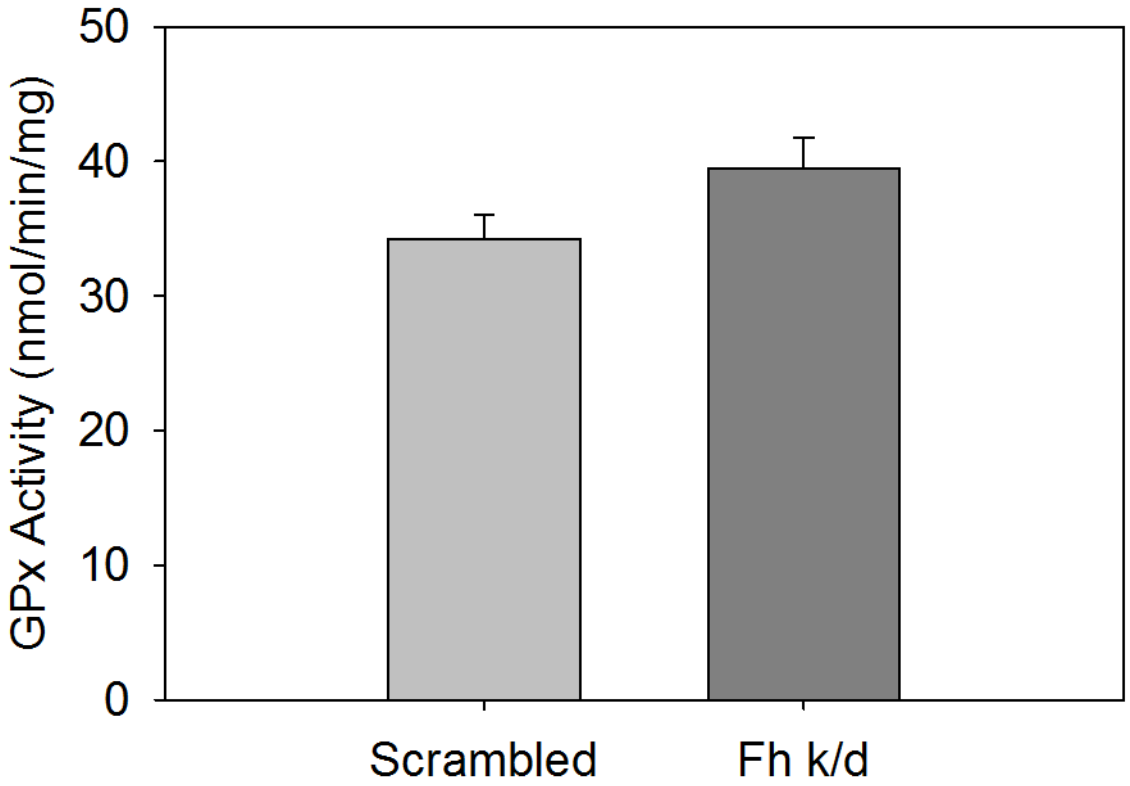

Figure 4.7: GPx activity in scrambled vs. *Fh* k/d 3T3-L1 fibroblasts. 3T3-L1 fibroblasts were transduced with a scrambled virus or viral shRNA that knocks-down fumarase (Fh). Cellular GPx activity was measured in lysates using a colorimetric GPx activity assay that utilizes glutathione (GSH), glutathione reductase (GR) and nicotinamide adenine dinucleotide phosphate (NADPH). GPx activity is expressed as the molar rate of NADPH oxidation per mL of protein (scrambled n=5, mean ± S.E.M.; *Fh* k/d n=5, mean ± S.E.M.). No significant differences were detected between scrambled and *Fh* k/d groups.

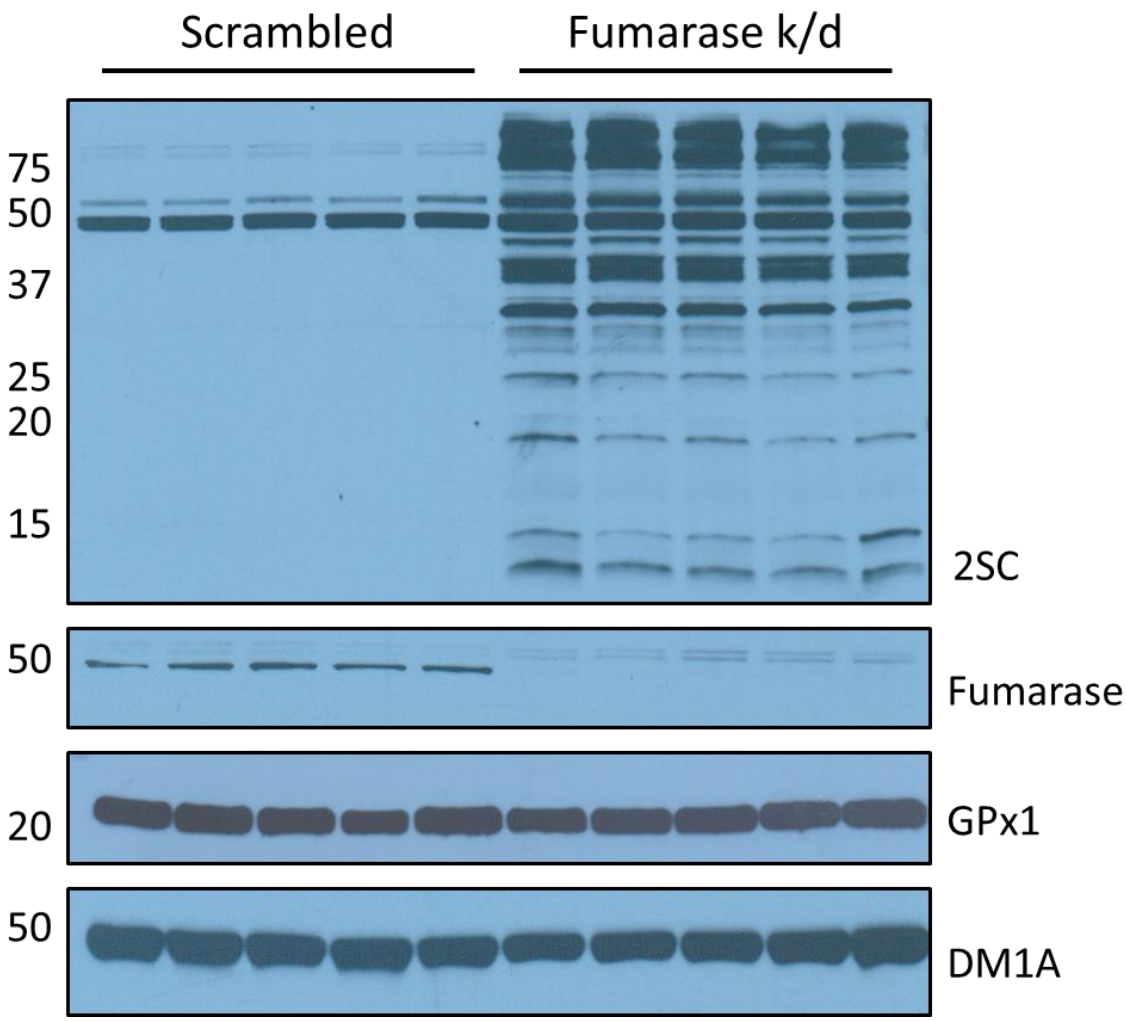

Figure 4.8: Western blot of GPx levels in scrambled vs. *Fh* k/d 3T3-L1 fibroblasts. 3T3-L1 fibroblasts were transduced with a scrambled virus or viral shRNA that knocks-down fumarase (Fh). Protein (30 µg) was separated using 1-D SDS-PAGE and detection of 2SC was performed using a polyclonal anti-2SC antibody. Western blotting was also used to analyze protein expression of GPx1 to determine if differences existed between the two groups, and to analyze levels of fumarase to confirm the knock-down in *Fh* k/d cells. MW markers are shown in kDa on the left and α-tubulin (DM1A) was used as a loading control.

```
        10         20         30         40         50
MCAAQRSAAA LAAAAPRTVY AFSARPLAGG EPFNLSSLRG KVLLIENVAS

        60         70         80         90        100
LUGTTVRDYT QMNDLQRRLG PRGLVVLGFP CNQFGHQENA KNEEILNCLK

       110        120        130        140        150
YVRPGGGFEP NFMLFEKCEV NGEKAHPLFA FLREVLPTPS DDATALMTDP

       160        170        180        190        200
KFITWSPVCR NDVSWNFEKF LVGPDGVPVR RYSRRFLTID IEPDIETLLS


QGASA
```

Source from <http://www.uniprot.org/uniprot/P00435>

Figure 4.9: Bovine erythrocyte GPx protein sequence. Protein sequence from bovine erythrocyte GPx (P00435). Sec is underlined at position 52.

CHAPTER 5

FUTURE DIRECTIONS

Our laboratory is interested in continuing to study the effects of fumarate and fumarate esters on selenocysteines. The results of this thesis indicate that thioredoxin reductase (TrxR) and its active site Sec may be more readily succinated by dimethyl fumarate than glutathione peroxidase (GPx), however, neither protein Sec residue appeared to react with endogenously produced fumarate as readily as we initially predicted. To further understand this we will continue a new collaboration with Dr. Gianluca Miglio (University of Turin, Italy) modeling how charges and substrate accessibility determine the likelihood of succination, based on available crystal structures of Sec-containing proteins. Although the *in vitro* experiments from this thesis identified dimethyl fumarate (DMF) as a new inhibitor of TrxR through proteomic analysis, we hope to continue these experiments to confirm that the selenocysteine (Sec) residue is in fact the target of succination by the drug and the reason for the observed decrease in enzymatic activity.

An immediate goal, following the completion of this thesis, is to continue with experiments to investigate the rapid reactivity of the DMF with cellular targets, as this drug is likely acting on a plethora of intracellular proteins. New efforts in our laboratory are underway to identify these targets and define the downstream effects of DMF. Ultimately it is hoped that these studies will help us better understand both the beneficial

actions, as well as the side effects of this drug, and facilitate the design of more targeted therapeutic strategies for the treatment of multiple sclerosis (MS). In our further investigation of the effects of DMF on TrxR, we plan to use an alternative commercially available activity assay (based on the reduction of insulin disulfides by reduced thioredoxin with thioredoxin reductase and NADPH) that will hopefully provide more reliable data for cellular TrxR activity in our N1E-115 model. Our goal is to determine the effects of DMF after 1 hour and 3 hours of treatment, while utilizing cycloheximide in various groups to inhibit protein synthesis. This will prevent the cells from synthesizing additional antioxidants such as TrxR1 in response to the insults from DMF, and we hypothesize that TrxR activity might be reduced. While we accept that GPx may not be succinated and inhibited by fumarate, the accessibility of the TrxR active site encourages us to pursue these planned studies with it to ensure that we have properly determined whether it can be modified by endogenously produced fumarate.

CHAPTER 6

METHODS AND MATERIALS

Materials

All chemicals were purchased from Sigma Aldrich (St. Louis, MO), unless otherwise noted. Preparation of anti-2SC antibody was performed as described (Nagai 2007) by Eurogentec (Fremont, CA). Polyvinylidene fluoride (PVDF) was purchased from GE Healthcare (Fairfield, CT). Tris Base, L-glycine, and sodium dodecyl sulfate (SDS) were purchased from Fisher Scientific (Waltham, MA). Tween-20 and Criterion™TGX™ Precast Gels were from Bio-Rad (Hercules, CA). Thioredoxin Reductase 1 (TrxR1) rat recombinant protein was purchased from IMCO (Stockholm, Sweden) and Glutathione Peroxidase Colorimetric Activity assay were purchased from Cayman Chemicals (Ann Arbor, MI).

Protein Extraction from Cells

All samples and reagents were kept on ice while protein was harvested. The cells were washed three times with phosphate buffered saline (PBS). The cells were collected in 50 mM Tris-HCl-EDTA assay buffer and homogenized on ice using a plastic homogenizer. The samples were then centrifuged at 10,000 g for 15 minutes at 4°C and the supernatant was collected. Activity assays were performed on cell lysate supernatants before being frozen at -70°C for future experiments.

Measurement of Thioredoxin Reductase 1 (TrxR1) Activity in Recombinant Samples after Treatment with Fumarate or Dimethyl Fumarate (DMF)

TrxR activity was measured in a clear 96-well (Corning) plate format using an adaptation of the method previously published (Holmgren et al., 2014). 1.5 μg of rat recombinant TrxR1 protein (Cayman Chemicals, Ann Arbor, MI) was added to each sample/enzymatic in 50 mM Tris-HCl-EDTA assay buffer. Each sample was pre-reduced with 30-35 μg of nicotinamide adenine dinucleotide phosphate (NADPH) for 5 minutes prior to addition of either fumarate (0-100 mM) or DMF (0-100 μM). The samples were left to incubate for varying time periods (1-18 hours) at either room temperature or 4°C. After incubation an additional 30-35 μg of NADPH was added to each enzymatic well, quickly followed by the addition of 5 mM 5,5'-dithio-*bis*(2-dinitrobenzoic acid) (DTNB) to initiate the reactions. Background/Non-enzymatic wells contained only Tris-HCl-EDTA assay buffer with DTNB and were subtracted from the absorbance values obtained for the wells containing protein. Final volumes in each well totaled 200 μL. Absorbances were measured at the 405 nm wavelength using a Tecan Safire^2 plate reader every minute for 5 minutes. Data was collected using XFluor4 software (a Microsoft Excel macro).

Measurement of Thioredoxin Reductase (TrxR) Activity in Cell Extracts

TrxR activity was measured in a clear 96-well (Corning) plate format using an adaptation of the method published by (45). Sample wells contained 100-400 μg of protein from cell lysates, 60-70 μg of NADPH, and 50 mM Tris-HCl-EDTA assay buffer, to a final volume of 200 μl. Replicate samples containing 20 μM of the TrxR inhibitor sodium aurothiomalate (ATM) were also prepared in some cases. Positive control wells

contained 1.5 μg of rat recombinant TrxR1, 60-70 μg NADPH, and 50 mM Tris-HCl-EDTA assay buffer. The enzymatic reactions were initiated by the addition of 5,5'-dithio-*bis*(2-dinitrobenzoic acid) DTNB to each well, after which the absorbance for each well was immediately measured at 405 nm every minute for 5 minutes using a Tecan Safire^2 plate reader. Background/Non-enzymatic wells contained only Tris-HCl-EDTA assay buffer with DTNB and were subtracted from the absorbance values obtained for the wells containing protein. Data was collected using XFluor4 software (a Microsoft Excel macro).

Measurement of Glutathione Peroxidase (GPx) Activity in Cell Lysates

GPx activity was measured in a clear 96-well (Corning) plate using a Glutathione Peroxidase colorimetric activity assay kit (Cayman Chemicals, Ann Arbor, MI), according to the manufacturer's instructions. Sample wells contained 15-18 μg of protein from cell lysates, 50 μL co-substrate mixture (containing NADPH, glutathione, and glutathione reductase), and 50 mM Tris-HCl-EDTA assay buffer. Positive control wells contained 20 μL of kit-supplied Bovine-erythrocyte GPx protein, 50 μL co-substrate mixture, and 100 μL Tris-HCl-EDTA assay buffer. Background/non-enzymatic wells contained 50 μL co-substrate mixture and 120 μL Tris-HCl-EDTA assay buffer. The enzymatic reactions were initiated by the addition of 20 μL of cumene hydroperoxide, after which the absorbance for each well was measured at 340 nm (monitoring the loss of NADPH) each minute for 5 minutes using a Tecan Safire^2 plate reader. Data was collected using XFluor4 software (a Microsoft Excel macro).

Western Immunoblotting

Samples were prepared using 30 μg for cell lysates with the addition of 5-7 μL 4X Laemmli loading buffer. The samples were then boiled at 95°C for 15 minutes, flash centrifuged then loaded onto 7.5%, 12%, or 18% agarose gels and electrophoresed at 200 V for 50-70 minutes. The protein was transferred to a PVDF membrane in transfer buffer at 250 mA for 100 minutes or 40 mA at 4°C. The membrane was Ponceau stained then washed 3 times for 5 minutes in 20 mM Tris-Glycine containing % Tween20 wash buffer, and blocked in 5% non-fat milk or 5% bovine serum albumin (BSA) if suggested by antibody manufacturer. Membranes were probed using primary rabbit polyclonal anti-2SC (1/8000). Antibodies against fumarase (Lot #1), TrxR2 (Lot #1) and DM1A tubulin (Lot #8) were from Cell Signaling Technology (Danvers, MA), GPx1 (Lot #GR82550-9) from Novus Biologicals (Littleton, CO), GPx4 (Lot #GR251529-3) from Abcam (Cambridge, MA), TrxR1 (Lot #CBZG021007) from R&D Systems (Minneapolis, MN). HRP-coupled secondary antibodies were used where appropriate; anti-mouse (Lot #X0328) from Vector Labs (Burlingame, CA) and anti-rabbit (Lot #26) from Cell signaling Technology (Danvers, MA). Pierce® ECL 2 Western Blotting Substrate was used prior to the detection of chemiluminescence using photographic film (Denville Scientific, Metuchen, NJ). ImageJ software (NIH) was used to quantify band intensity by densitometry.

In-Gel Protein Digestion

Recombinant rat thioredoxin reductase 1 (TrxR1) was incubated in the absence or presence of 100 μM DMF for 20 hours at 37°C. Following incubation, 3 μg of protein

was electrophoresed by SDS-PAGE as described (section above). Following electrophoresis the gel was stained with Coomassie Brilliant Blue for 1 hour, followed by de-staining in 7% acetic acid/10% methanol for 24 hours to detect TrxR protein. The excised gel bands cut into several smaller pieces before being washed in a 50/50% methanol/acetic acid solution for several days to completely remove Coomassie stain. Gel bands were then washed in 50mM ammonium bicarbonate in 50% acetonitrile, then 100% acetonitrile for 5 mins and allowed to dry using a SpeedVac centrifuge. Sample was reduced with 10 mM dithiothreitol (DTT) was and then alkylated using 170 mM 4-vinylpyridine (4-VP). Trypsin digestion was carried out overnight at 37°C in the presence of 1.5 ng sequence grade modified trypsin (Promega, Madison, WI) in 50 mM ammonium bicarbonate. The supernatant and extracts with 5% formic acid in 50% acetonitrile, then 100% acetonitrile and were pooled and dried down in a SpeedVac centrifuge to ~20 µL. The digested samples were analyzed on a Dionex Ultimate 3000-LC system (Thermo Scientific, Rockford, IL) coupled to a Velos Pro Orbitrap mass spectrometer (Thermo Scientific, Rockford, IL).

Data Analysis

All graphs were generated in Sigmaplot 11. Statistical analyses of the data were performed on SigmaStat software (Sigmaplot 11, San Jose, CA). All data were plotted as means ± S.E.M. An unpaired Student *t* test was used to test for statistical differences between two sets of data. A One Way ANOVA using Holm-Sidak test was used when comparing 3 or more sets of data. Differences were considered statistically significant at $^{*}p<0.05$.

REFERENCES

1. Friedman M, Finley J W, Yeh L S. Relative nucleophilic reactivities of amino groups and mercaptide ions in addition reactions with alpha, beta-unsaturated compounds. *J. Amer. Chem. Soc.* 1965; 87:3572-3682

2. Frizzell N, Lima M, Baynes JW. Succination of proteins in diabetes. *Free Radic Res.* 2011; 45(1):101-109.

3. Bulaj G, Kortemme T, Goldenberg DP. Ionization-reactivity relationships for cysteine thiols in polypeptides. *Biochemistry.* 1998; 37(25):8965-72.

4. Finkel T. Signal transduction by reactive oxygen species. *J Cell Biol*. 2011; 194(1):7-15.

5. Hoffman S, Nolin J, Mcmillan D, Wouters E, Janssen-heininger Y, Reynaert N. Thiol redox chemistry: role of protein cysteine oxidation and altered redox homeostasis in allergic inflammation and asthma. *J Cell Biochem.* 2015; 116(6):884-892.

6. Merkley ED, Metz TO, Smith RD, Baynes JW, Frizzell N. The succinated proteome. *Mass Spectrom Rev.* 2014; 33(2):98-109.

7. Alderson NL, Wang Y, Blatnik M, et al. S-(2-Succinyl)cysteine: a novel chemical modification of tissue proteins by a Krebs cycle intermediate. *Arch Biochem Biophys.* 2006; 450(1):1-8.

8. Blatnik M, Frizzell N, Thorpe SR, Baynes JW. Inactivation of glyceraldehyde-3-phosphate dehydrogenase by fumarate in diabetes: formation of S-(2-succinyl)cysteine, a novel chemical modification of protein and possible biomarker of mitochondrial stress. *Diabetes*. 2008; 57(1):41-49.

9. Ternette N, Yang M, Laroyia M, Kitagawa M, O'Flaherty L, Wolhulter K, Igarashi K, Saito K, Kato K, Fischer R, Berquand A, Kessler BM, Lappin T, Frizzell N, Soga T, Adam J, Pollard PJ. Inhibition of mitochondrial aconitase by succination in fumarate hydratase deficiency. *Cell Rep*. 2013; 3(3):689-700.

10. Du X, Matsumura T, Edelstein D, Rossetti L, Zsengellér Z, Szabó C, Brownlee M. Inhibition of GAPDH activity by poly(ADP-ribose) polymerase activates three major pathways of hyperglycemic damage in endothelial cells. *J Clin Invest*. 2003; 112(7):1049-1057.

11. Pajvani UB, Hawkins M, Combs TP, Rajala MW, Doebber T, Berger JP, Wagner JA, Wu M, Knopps A, Xiang AH, Utzschneider KM, Kahn SE, Olefsky JM, Buchanan TA, Scherer PE. Complex distribution, not absolute amount of adiponectin, correlates with thiazolidinedione-mediated improvement in insulin sensitivity. *J Biol Chem*. 2004; 279(13):12152-12162.

12. Frizzell N, Rajesh M, Jepson MJ, Nagai R, Carson JA, Thorpe SR. Succination of thiol groups in adipose tissue proteins in diabetes: succination inhibits polymerization and secretion of adiponectin. *J Biol Chem*. 2009; 284(38):25772-25781.

13. Frizzell N, Thomas SA, Carson JA, Baynes JW. Mitochondrial stress causes increased succination of proteins in adipocytes in response to glucotoxicity. *Biochem J*. 2012; 445(2):247-254.

14. Thomas SA, Storey KB, Baynes JW, Frizzell N. Tissue distribution of S-(2-succino)cysteine (2SC), a biomarker of mitochondrial stress in obesity and diabetes. *Obesity (Silver Spring)*. 2012; 20(2):263-269.

15. Chen YB, Brannon AR, Toubaji A, Dudas ME, Won HH, Al-Ahmadie HA, Fine SW, Gopalan A, Frizzell N, Voss MH, Russo P, Berger MF, Tickoo SK, Reuter VE. Hereditary leiomyomatosis and renal cell carcinoma syndrome-associated renal cancer: recognition of the syndrome by pathologic features and the utility of detecting aberrant succination by immunohistochemistry. *Am J Surg Pathol*. 2014; 38(5):627-637.

16. Yang M, Ternette N, Su H, Dabiri R, Kessler BM, Adam J, The BT, Pollard PJ. The Succinated Proteome of FH-Mutant Tumours. *Metabolites*. 2014; 4(3):640-654.

17. Reyes C, Karamurzin Y, Frizzell N, Garg K, Nonaka D, Chen YB, Soslow RA. Uterine smooth muscle tumors with features suggesting fumarate hydratase aberration: detailed morphologic analysis and correlation with S-(2-succino)-cysteine immunohistochemistry. *Mod Pathol*. 2014; 27(7):1020-1027.

18. Joseph NM, Solomon DA, Frizzell N, Rabban JT, Zaloudek C, Garg K. Morphology and Immunohistochemistry for 2SC and FH Aid in Detection of Fumarate Hydratase Gene Aberrations in Uterine Leiomyomas From Young Patients. *Am J Surg Pathol*. 2015; 39(11):1529-1539.

19. Piroli GG, Manuel AM, Clapper AC, Walla MD, Baatz JE, Palmiter RD, Quintana A, Frizzell N. Succination is Increased on Select Proteins in the Brainstem of the NADH dehydrogenase (ubiquinone) Fe-S protein 4 (Ndufs4) Knockout Mouse, a Model of Leigh Syndrome. *Mol Cell Proteomics*. 2016; 15(2):445-461.

20. Donovan J, Copeland PR. Selenocysteine insertion sequence binding protein 2L is implicated as a novel post-transcriptional regulator of selenoprotein expression. *PLoS ONE*. 2012; 7(4):e35581.

21. Huber RE, Criddle RS. Comparison of the chemical properties of selenocysteine and selenocystine with their sulfur analogs. *Arch Biochem Biophys*. 1967; 122(1):164-173.

22. Arnér ES. Selenoproteins-What unique properties can arise with selenocysteine in place of cysteine?. *Exp Cell Res*. 2010; 316(8):1296-1303.

23. Kryukov GV, Castellano S, Novoselov SV, Lobanov AV, Zehtab O, Guigó R, Gladyshev VN. Characterization of mammalian selenoproteomes. *Science*. 2003; 300(5624):1439-1443.

24. Labunskyy VM, Hatfield DL, Gladyshev VN. Selenoproteins: molecular pathways and physiological roles. *Physiol Rev*. 2014; 94(3):739-777.

25. Reeves MA, Hoffmann PR. The human selenoproteome: recent insights into functions and regulation. *Cell Mol Life Sci*. 2009; 66(15):2457-2478.

26. Pitts MW, Byrns CN, Ogawa-wong AN, Kremer P, Berry MJ. Selenoproteins in nervous system development and function. *Biol Trace Elem Res*. 2014; 161(3):231-245.

27. Anttonen AK, Hilander T, Linnankivi T, Isohanni P, French RL, Liu Y, Simonović , Söll D1, Somer M, Muth-Pawlak D, Corthals GL, Laari A, Ylikallio E, Lähde M, Valanne L, Lönnqvist T, Pihko H, Paetau A, Lehesjoki AE, Suomalainen A, Tyynismaa H. Selenoprotein biosynthesis defect causes progressive encephalopathy with elevated lactate. *Neurology*. 2015; 85(4):306-315.

28. Byrns CN, Pitts MW, Gilman CA, Hashimoto AC, Berry MJ. Mice lacking selenoprotein P and selenocysteine lyase exhibit severe neurological dysfunction, neurodegeneration, and audiogenic seizures. *J Biol Chem*. 2014; 289(14):9662-9674.

29. Ray PD, Huang BW, Tsuji Y. Reactive oxygen species (ROS) homeostasis and redox regulation in cellular signaling. *Cell Signal*. 2012; 24(5):981-990.

30. Finkel T. Signal transduction by reactive oxygen species. *J Cell Biol*. 2011; 194(1):7-15.

31. Park J, Min JS, Kim B, Chae UB, Yun JW, Choi MS, Kong KT, Lee DS. Mitochondrial ROS govern the LPS-induced pro-inflammatory response in microglia cells by regulating MAPK and NF-κB pathways. *Neurosci Lett*. 2015; 584:191-196.

32. Wei M, Li Z, Xiao L, Yang Z. Effects of ROS-relative NF-κB signaling on high glucose-induced TLR4 and MCP-1 expression in podocyte injury. *Mol Immunol*. 2015; 68(2 Pt A):261-271.

33. Betteridge DJ. What is oxidative stress?. *Metab Clin Exp*. 2000; 49(2 Suppl 1):3-8.

34. Valko M, Leibfritz D, Moncol J, Cronin MT, Mazur M, Telser J. Free radicals and antioxidants in normal physiological functions and human disease. *Int J Biochem Cell Biol.* 2007; 39(1):44-84.

35. Brownlee M. Biochemistry and molecular cell biology of diabetic complications. *Nature*. 2001; 414(6865):813-820.

36. Lin Y, Berg AH, Iyengar P, Lam TK, Giacca A, Combs TP, Rajala MW, Du X, Rollman B, Li W, Hawkins M, Barzilai N, Rhodes CJ, Fantus IG, Brownlee M, Scherer PE. The hyperglycemia-induced inflammatory response in adipocytes: the role of reactive oxygen species. *J Biol Chem*. 2005; 280(6):4617-4626.

37. Anderson EJ, Lustig ME, Boyle KE, Woodlief TL, Kane DA, Lin CT, Price JW 3rd, Kang L, Rabinovitch PS, Szeto HH, Houmard JA, Cortright RN, Wasserman DH, Neufer PD. Mitochondrial H2O2 emission and cellular redox state link excess fat intake to insulin resistance in both rodents and humans. *J Clin Invest*. 2009; 119(3):573-581.

38. Peng X, Mandal PK, Kaminskyy VO, Lindqvist A, Conrad M, Arnér ES. Sec-containing TrxR1 is essential for self-sufficiency of cells by control of glucose-derived H2O2. *Cell Death Dis*. 2014; 5:e1235.

39. Arnér ES, Holmgren A. Physiological functions of thioredoxin and thioredoxin reductase. *Eur J Biochem*. 2000; 267(20):6102-6109.

40. Papp LV, Lu J, Holmgren A, Khanna KK. From selenium to selenoproteins: synthesis, identity, and their role in human health. *Antioxid Redox Signal*. 2007; 9(7):775-806.

41. Lee S, Kim SM, Lee RT. Thioredoxin and thioredoxin target proteins: from molecular mechanisms to functional significance. *Antioxid Redox Signal*. 2013; 18(10):1165-1207.

42. Arnér ES, Holmgren A. The thioredoxin system in cancer. *Semin Cancer Biol*. 2006; 16(6):420-426.

43. Lu J, Zhong L, Lönn ME, Burk RF, Hill KE, Holmgren A. Penultimate selenocysteine residue replaced by cysteine in thioredoxin reductase from selenium-deficient rat liver. *FASEB J*. 2009; 23(8):2394-2402.

44. Biterova EI, Turanov AA, Gladyshev VN, Barycki JJ. Crystal structures of oxidized and reduced mitochondrial thioredoxin reductase provide molecular details of the reaction mechanism. *Proc Natl Acad Sci USA*. 2005; 102(42):15018-15023.

45. Fang J, Lu J, Holmgren A. Thioredoxin reductase is irreversibly modified by curcumin: a novel molecular mechanism for its anticancer activity. *J Biol Chem*. 2005; 280(26):25284-25290.

46. Fang J, Holmgren A. Inhibition of thioredoxin and thioredoxin reductase by 4-hydroxy-2-nonenal in vitro and in vivo. *J Am Chem Soc*. 2006; 128(6):1879-1885.

47. Lushchak VI. Glutathione homeostasis and functions: potential targets for medical interventions. *J Amino Acids*. 2012; 2012:736837.

48. Toppo S, Flohé L, Ursini F, Vanin S, Maiorino M. Catalytic mechanisms and specificities of glutathione peroxidases: variations of a basic scheme. *Biochim Biophys Acta*. 2009; 1790(11):1486-1500.

49. Flohé, L. The selenoprotein glutathione peroxidase. *Glutathione: Chemical, Biochemical, and Medical Aspects-Part A*. 1989; 643–731.

50. Flohé L, Toppo S, Cozza G, Ursini F. A comparison of thiol peroxidase mechanisms. *Antioxid Redox Signal*. 2011; 15(3):763-780.

51. Brigelius-Flohé R, Maiorino M. Glutathione peroxidases. *Biochim Biophys Acta*. 2013; 1830(5):3289-3303.

52. Flohe L, Günzler WA, Schock HH. Glutathione peroxidase: a selenoenzyme. *FEBS Lett*. 1973; 32(1):132-134.

53. Lubos E, Loscalzo J, Handy DE. Glutathione peroxidase-1 in health and disease: from molecular mechanisms to therapeutic opportunities. *Antioxid Redox Signal*. 2011; 15(7):1957-1997.

54. Ford HL, Gerry E, Johnson M, Williams R. A prospective study of the incidence, prevalence and mortality of multiple sclerosis in Leeds. *J Neurol*. 2002; 249(3):260-265.

55. Keegan BM, Noseworthy JH. Multiple sclerosis. *Annu Rev Med*. 2002; 53:285-302.

56. Ascherio A, Munger KL, Lünemann JD. The initiation and prevention of multiple sclerosis. *Nat Rev Neurol*. 2012; 8(11):602-612.

57. www.nationalmssociety.org

58. Moharregh-khiabani D, Linker RA, Gold R, Stangel M. Fumaric Acid and its esters: an emerging treatment for multiple sclerosis. *Curr Neuropharmacol*. 2009; 7(1):60-64.

59. Ghoreschi K, Brück J, Kellerer C, Deng C, Peng H, Rothfuss O, Hussain RZ, Gocke AR, Respa A, Glocova I, Valtcheva N, Alexander E, Feil S, Feil R, Schulze-Osthoff K, Rupec RA, Lovett-Racke AE, Dringen R, Racke MK, Röcken M. Fumarates improve psoriasis and multiple sclerosis by inducing type II dendritic cells. *J Exp Med*. 2011; 208(11):2291-2303.

60. Mrowietz U, Christophers E, Altmeyer P. Treatment of psoriasis with fumaric acid esters: results of a prospective multicentre study. German Multicentre Study. *Br J Dermatol*. 1998; 138(3):456-460.

61. Nibbering PH, Thio B, Zomerdijk TP, Bezemer AC, Beijersbergen RL, van Furth R. Effects of monomethylfumarate on human granulocytes. *J Invest Dermatol*. 1993; 101(1):37-42.

62. Havrdova E, Hutchinson M, Kurukulasuriya NC, Raghupathi K, Sweetser MT, Dawson KT, Gold R. Oral BG-12 (dimethyl fumarate) for relapsing-remitting multiple sclerosis: a review of DEFINE and CONFIRM. Evaluation of: Gold R, Kappos L, Arnold D, et al. Placebo-controlled phase 3 study of oral BG-12 for relapsing multiple sclerosis. N Engl J Med 2012;367:1098-107; and Fox RJ, Miller DH, Phillips JT, et al. Placebo-controlled phase 3 study of oral BG-12 or glatiramer in multiple sclerosis. N Engl J Med 2012;367:1087-97. *Expert Opin Pharmacother*. 2013; 14(15):2145-2156.

63. Kappos L, Gold R, Arnold DL, Bar-Or A, Giovannoni G, Selmaj K, Sarda SP, Agarwal S, Zhang A, Sheikh SI, Seidman E, Dawson KT. Quality of life outcomes with BG-12 (dimethyl fumarate) in patients with relapsing-remitting multiple sclerosis: the DEFINE study. *Mult Scler*. 2014; 20(2):243-252.

64. Lee DH, Stangel M, Gold R, Linker RA. The fumaric acid ester BG-12: a new option in MS therapy. *Expert Rev Neurother*. 2013; 13(8):951-958.

65. Lee MA, Smith S, Palace J, Matthews PM. Defining multiple sclerosis disease activity using MRI T2-weighted difference imaging. *Brain*. 1998; 121 (Pt 11):2095-2102.

66. Venci JV, Gandhi MA. Dimethyl fumarate (Tecfidera): a new oral agent for multiple sclerosis. *Ann Pharmacother*. 2013; 47(12):1697-1702.
67. Scannevin RH, Chollate S, Jung MY, Shackett M, Patel H, Bista P, Zeng W, Ryan S, Yamamoto M, Lukashev M, Rhodes KJ. Fumarates promote cytoprotection of central nervous system cells against oxidative stress via the nuclear factor (erythroid-derived 2)-like 2 pathway. *J Pharmacol Exp Ther*. 2012; 341(1):274-284.

68. Linker RA, Lee DH, Ryan S, van Dam AM, Conrad R, Bista P, Zeng W, Hronowsky X, Buko A, Chollate S, Ellrichmann G, Brück W, Dawson K, Goelz S, Wiese S, Scannevin RH, Lukashev M, Gold R. Fumaric acid esters exert neuroprotective effects in neuroinflammation via activation of the Nrf2 antioxidant pathway. *Brain*. 2011; 134(Pt 3):678-692.

69. Johnson JA, Johnson DA, Kraft AD, Calkins MJ, Jakel RJ, Vargas MR, Chen PC. The Nrf2-ARE pathway: an indicator and modulator of oxidative stress in neurodegeneration. *Ann N Y Acad Sci*. 2008; 1147:61-69.

70. Lehmann JC, Listopad JJ, Rentzsch CU, Igney FH, von Bonin A, Hennekes HH, Asadullah K, Docke WD. Dimethylfumarate induces immunosuppression via glutathione depletion and subsequent induction of heme oxygenase 1. *J Invest Dermatol*. 2007; 127(4):835-845.

71. Schmidt TJ, Ak M, Mrowietz U. Reactivity of dimethyl fumarate and methylhydrogen fumarate towards glutathione and N-acetyl-L-cysteine--preparation of S-substituted thiosuccinic acid esters. *Bioorg Med Chem*. 2007; 15(1):333-342.

72. Gold R, Giovannoni G, Phillips JT, Fox RJ, Zhang A, Meltzer L, Kurukulasuriya NC. Efficacy and safety of delayed-release dimethyl fumarate in patients newly diagnosed with relapsing-remitting multiple sclerosis (RRMS). *Mult Scler*. 2015; 21(1):57-66.

73. Lin SX, Lisi L, Dello Russo C, Polak PE, Sharp A, Weinberg G, Kalinin S, Feinstein DL. The anti-inflammatory effects of dimethyl fumarate in astrocytes involve glutathione and heme oxygenase-1. *ASN Neuro*. 2011; 3(2)

74. Manuel AM, Frizzell N. Adipocyte protein modification by Krebs cycle intermediates and fumarate ester-derived succination. *Amino Acids*. 2013; 45(5):1243-1247.

75. Piroli GG, Manuel AM, Walla MD, Jepson MJ, Brock JW, Rajesh MP, Tanis RM, Cotham WE, Frizzell N. Identification of protein succination as a novel modification of tubulin. *Biochem J*. 2014; 462(2):231-245.

76. Cai W, Zhang L, Song Y, Wang B, Zhang B, Cui X, Hu G, Liu Y, Wu J, Fang J. Small molecule inhibitors of mammalian thioredoxin reductase. *Free Radic Biol* Med. 2012; 52(2):257-265.
77. Saccoccia F, Angelucci F, Boumis G, Carotti D, Desiato G, Miele AE, Bellelli A. Thioredoxin reductase and its inhibitors. *Curr Protein Pept Sci*. 2014; 15(6):621-646.

78. Zhao R, Masayasu H, Holmgren A. Ebselen: a substrate for human thioredoxin reductase strongly stimulating its hydroperoxide reductase activity and a superfast thioredoxin oxidant. *Proc Natl Acad Sci USA*. 2002; 99(13):8579-8584.

79. Engman L, Cotgreave I, Angulo M, Taylor CW, Paine-murrieta GD, Powis G. Diaryl chalcogenides as selective inhibitors of thioredoxin reductase and potential antitumor agents. *Anticancer Res*. 1997; 17(6D):4599-4605.

80. Zhang J, Li Y, Duan D, Yao J, Gao K, Fang J. Inhibition of thioredoxin reductase by alantolactone prompts oxidative stress-mediated apoptosis of HeLa cells. *Biochem Pharmacol*. 2016; 102:34-44.

81. Yao XF, Zheng BL, Bai J, Jiang LP, Zheng Y, Qi BX, Geng CY, Zhong LF, Yang G, Chen M, Liu XF, Sun XC. Low-level sodium arsenite induces apoptosis through inhibiting TrxR activity in pancreatic β-cells. *Environ Toxicol Pharmacol*. 2015; 40(2):486-491.

82. Nagai R, Brock JW, Blatnik M, Baatz JE, Bethard J, Walla MD, Thorpe SR, Baynes JW, Frizzell N. Succination of protein thiols during adipocyte maturation: a biomarker of mitochondrial stress. *J Biol Chem*. 2007; 282(47):34219-34228.

83. Holmgren A. Thioredoxin. *Annu Rev Biochem*. 1985; 54:237-271.

84. Itoh K, Mimura J, Yamamoto M. Discovery of the negative regulator of Nrf2, Keap1: a historical overview. *Antioxid Redox Signal*. 2010; 13(11):1665-1678.

85. Kensler TW, Wakabayashi N, Biswal S. Cell survival responses to environmental stresses via the Keap1-Nrf2-ARE pathway. *Annu Rev Pharmacol Toxicol*. 2007; 47:89-116.

86. Osburn WO, Kensler TW. Nrf2 signaling: an adaptive response pathway for protection against environmental toxic insults. *Mutat Res*. 2008; 659(1-2):31-39.

87. Chaudiere J, Wilhelmsen EC, Tappel AL. Mechanism of selenium-glutathione peroxidase and its inhibition by mercaptocarboxylic acids and other mercaptans. *J Biol Chem*. 1984; 259(2):1043-1050.

88. Bosch-morell F, Flohé L, Marín N, Romero FJ. 4-Hydroxynonenal inhibits glutathione peroxidase: protection by glutathione. *Free Radic Biol Med*. 1999; 26(11-12):1383-1387.

89. Asahi M, Fujii J, Takao T, et al. The oxidation of selenocysteine is involved in the inactivation of glutathione peroxidase by nitric oxide donor. *J Biol Chem*. 1997; 272(31):19152-19157.

90. Pacher P, Beckman JS, Liaudet L. Nitric oxide and peroxynitrite in health and disease. *Physiol Rev*. 2007; 87(1):315-424.

91. Ladenstein R, Epp O, Bartels K, Jones A, Huber R, Wendel A. Structure analysis and molecular model of the selenoenzyme glutathione peroxidase at 2.8 A resolution. *J Mol Biol*. 1979; 134(2):199-218.

92. Liu X, Pietsch KE, Sturla SJ. Susceptibility of the antioxidant selenoenyzmes thioredoxin reductase and glutathione peroxidase to alkylation-mediated inhibition by anticancer acylfulvenes. *Chem Res Toxicol*. 2011; 24(5):726-736.

93. Xu Q, Hahn WS, Bernlohr DA. Detecting protein carbonylation in adipose tissue and in cultured adipocytes. *Meth Enzymol*. 2014; 538:249-61.

APPENDIX A

BUFFER PREPARATIONS

Assay Buffer

The buffer was prepared in 250 mL stocks containing 50 mM Tris-HCl pH 7.5, 150 mM NaCl, 1 mM EDTA. The buffer was stored at 4^{o}C.

Running Buffer

One liter of 10x stock was prepared containing 250 mM Tris-HCl, 1920 mM glycine and 10% (SDS).

Transfer Buffer

One liter of 10X stock was prepared containing 250 mM Tris-HCl, 1920 mM glycine. Methanol was added at 20% for transfer process.

Wash Buffer

One liter of 10X stock was prepared containing 200 mM Tris-HCl, pH 7.4. Tween-20 was added at 0.05% to 1X was buffer.

APPENDIX B

LOWRY ASSAY

Pipette the specific amounts of reagents into the microplate in the order listed. All samples are prepared in duplicates.

Table B.1: Preparation of BSA standard curve for the Lowry assay.

Probe	BSA (µL)	H20 (µL)	Copper Reagent (µL)	Incubation	Folin-Ciocolateu (µL)	Incubation
Blank	0	20	20	20 minutes at 37°C	60	30 minutes at 37°C
1	1	19	20		60	
2	2	18	20		60	
3	3	17	20		60	
4	4	16	20		60	
5	8	12	20		60	
6	10	10	20		60	
7	20	0	20		60	
Sample	5	15	20		60	

Stock BSA

Dissolve 50 mg BSA (Bovine Serum Albumin) in 10 mL deionized water=5 mg/mL stock/working solution

Working Solutions: Dilute 400 µL of 5 mg/mL stock in 600 µL water=2 mg/mL solution

Table B.2: Preparation of copper reagent for Lowry assay.

Stock Solution	**Working Solution**
Copper Sulfate 1% (w:v)	100 µL
Sodium Tartrate 2% (w:v)	100 µL
Sodium Carbonate 10% (w:v) in 0.5 M NaOH	2 mL

Folin-Ciocolateu Phenol Reagent: Purchased as a 2 N stock solution. For working solution at 500 µL of stock solution to 5.5 mL of water

Read absorbance at 660nm.

APPENDIX C

WESTERN BLOTTING

Gel Electrophoresis

1. After determining the protein content from the Lowry assay, 30-40 µg of protein was dissolved in water and 5 µL of Laemmli loading buffer was added.

2. Boil the samples for 15 min at 95°C then flash centrifuge.

3. Remove tape and comb from Bio-Rad pre cast Criterion gel and place in cassette.

4. Fill the cassette tank and gel with Tris/Glycine/SDS running buffer.

5. Load the samples into their individual lanes and 8 µL of marker into your lane of choice.

6. Run the gel at 200 V for 60 min.

Wet Transfer

1. Remove the gel from the pre-cast and cut to size

2. Soak the gel in Tris/Glycine/Methanol transfer buffer for 15 min.

3. Charge the PVDF membrane for ~30 sec in methanol. Soak the 2 pieces of blotting paper, 2 sponges, and the membrane in Tris/Glycine/methanol for 15 min.

4. Assemble the transfer apparatus, starting with the black side first. Keep all materials soaking in transfer buffer during the assembly.

5. Place the sponge flat on the black side, followed by a piece of blotting paper. Next, place the gel on top followed by the PVDF membrane. Roll out any air bubbles between the gel and membrane using a roller. Finally, put the remaining piece of blotting paper on top of the membrane and the sponge on top.

6. Assemble the apparatus and transfer at 250 mA for 100 min or 40 mA for at least 12 hrs.

7. Remove the membrane from the apparatus and wash 3 times with nanopure water. 8. Place the membrane in ponceau stain for 5 min then wash with nanopure water to visualize the bands. Inspect the membrane for equal loading and where bubbles formed during the transfer process. Wash the ponceau stain off the membrane with Tris-HCl wash buffer.

9. Block the membrane in 5% non-fat dry milk or 5% BSA for at least 1hr.

Immunostaining for 2SC

1. Prepare 1% milk by diluting the 5% milk 1:4 in Tris-HCl wash buffer.

2. Add 2SC antibody to the milk in a 1:5000 dilution. Incubate for at least 1 hr on the rocker.

3. Pour off the antibody and wash the membrane 3 times in wash buffer for 5 min each.

4. Add secondary antibody anti-rabbit to 1% milk, 1:15000 dilution and incubate for 1hr at room temperature.

5. Pour off the milk and was the membrane 3 times for 5 min each in wash buffer.

Developing

1. Prepare ECL solution by adding solution B to solution A and in a 1:40 dilution.

2. Add the ECL to the membrane and incubate for 5 min. Place the membrane in the cassette and cover with plastic wrap.

3. In the dark room, place a piece of X-ray film over the membrane then develop. Inspect the film after it has developed and adjust the exposure times accordingly.

Buffers

1. Stock Running Buffer: 10X SDS – 30.3 g Tris base, 144 g glycine and 10 g SDS dissolved to 1 L water
   - Working solution=100mL of 10X stock diluted to 1L water
2. Stock Transfer Buffer: 10X transfer – 30.3 g Tris base and 144 g glycine dissolved to 1 L water
   - Working solution=150 mL of 10X stock and 300 mL of methanol diluted to 1 L water
3. Stock Wash Buffer: 10X Wash – 24.4 g Tris base dissolved to 1 L water, pH 7.4

- Working solution=100 mL of 10X stock and 500 µL Tween-20 diluted to 1 L water

APPENDIX D

CELL CULTURE

3T3-L1 Cell Culture:

3T3-L1 murine fibroblasts were purchased from American Type Culture Collection (Manassas, VA) and maintained in DMEM containing 5 mM glucose, 10% Bovine Calf Serum (Thermo Scientific), 1% penicillin/streptomycin (CellGro) at 37°C with 5% CO_2 and 95% humidity. Growth medium was replaced every 2 days. At 70-80% confluence the cells were removed with trypsin (Thermo Scientific), neutralized with excess growth medium, and collected by centrifugation at 1000 g for 5 min. The cells were then re-suspended in growth medium for a new passage. 3T3-L1 fibroblasts were seeded at a density of 100,000 cells per 10 cm^2 petri dish. 3T3-L1 fibroblasts were induced to differentiate when the fibroblasts reached 24 hours post-confluence (~3-4 days) in DMEM with 10% Fetal Bovine Serum (Atlanta Biologicals), 1% penicillin/streptomycin, insulin (10 µg/mL), dexamethasone (0.3 µM), 3-isobutyl-1-methylxanthine (0.5 mM) and 30 mM glucose for 3 days. At day 0, differentiation medium was removed, cells were washed with PBS and maturation medium containing 5 mM/0.3 nM or 30 mM/3 nM glucose/insulin was applied. The medium was changed every 2 days and the adipocytes were matured in 5 mM or 30 mM glucose for 8 days Cells cultured in 5 mM glucose were supplemented with 5 mM glucose daily and several hours prior to protein harvest to maintain glucose levels. In order to generate a model of

maximal succination, 3T3-L1 fibroblasts were transduced with a lentivirus containing either *fumarase* (Fh) shRNA or scrambled control shRNA as described (Frizzell et al., 2015). The transduced cells exhibiting Fh knockdown were selected for and maintained in medium containing 1 μg/mL puromycin for 3 days prior to protein harvesting.

N1E Neuronal Culture:

N1E-115 cells (subclone N1E-115-1 neuroblastoma cells) were obtained from Sigma (08062511, St. Louis, MO). The cells were grown in non-differentiation medium (NDM, 90% DMEM (Gibco, Grand Island, NY) with 25 mM glucose, no pyruvate, 25 mM HEPES, 4 mM Glutamine) and 10% Foetal Bovine Serum (Atlanta Biologicals, Atlanta, GA) in 25 cm^2 flasks. When confluent the N1E-115 cells were differentiated into neurons in the presence of 2% FBS and 1.25% DMSO in DMEM. The differentiation was confirmed visually by phase contrast microscopy. The cells were treated with x dimethylfumarate for either 3 or 24 hrs prior to harvesting in 50 mM Tris-HCl-EDTA to assess thioredoxin reductase activity.